AN ABSTRACT OF THE THESIS OF

LEONARD LEROY HOVEY for the DOCTOR OF PHILOSOPHY
(Name) (Degree)

in CHEMICAL ENGINEERING presented on August 13, 1970
(Major) (Date)

Title: SURFACE RENEWAL RATE FOR THE ABSORPTION OF ODORIFEROUS SULFUR COMPOUNDS IN A WETTED WALL COLUMN

Redacted for Privacy

Abstract approved: _____
C. E. Wicks

Mass transfer coefficients for the odoriferous sulfur compounds produced by paper mills were measured in an externally wetted, wetted wall column. The gas phase mass transfer coefficients for methyl mercaptan and dimethyl sulfide were measured directly for gas Reynolds numbers of one to ten when using a reacting liquid solution to reduce the liquid phase resistance to mass transfer. Aqueous sodium hydroxide and cupric sulfate were found to be effective reacting liquids for the methyl mercaptan. Mercuric chloride was found to be an effective reacting liquid for reducing the liquid phase resistance to mass transfer for the dimethyl sulfide. The liquid mass transfer coefficients for methyl mercaptan, dimethyl sulfide, dimethyl disulfide, and sulfur dioxide in water were calculated for liquid Reynolds number of 200 to 1200.

The literature data for the vapor-liquid equilibrium of the methyl mercaptan-water system were reviewed and a six-fold variation noted. The published data for the equilibrium of the dimethyl sulfide-water and the dimethyl disulfide-water systems were found to be unsatisfactory for design. Henry's law constants based on concentration in moles per volume in both the liquid and gas were recommended for the three odoriferous gases studied.

The surface renewal penetration model was postulated for the system and found to be a satisfactory model for flows as low as a gas Reynolds number of one and for flows as high as a liquid Reynolds number of 1200. It was found that the surface renewal rate could be described by the equation $s = (1.77 \times 10^{-2})\nu^{1/3} N_{Re}^{1.39}$, ν in ft^2/sec and s in sec^{-1}. This equation was found to apply to both the gas and the liquid phases for the systems studied which include a gas Reynolds number range of 1 to 10 and a liquid Reynolds number range of 200 to 1200. This equation also fit the data published for absorbing carbon dioxide and oxygen into water in an internally wetted column for liquid Reynolds numbers of 1500 to 8500.

Surface Renewal Rate for the Absorption of Odoriferous Sulfur Compounds in a Wetted Wall Column

by

Leonard LeRoy Hovey

A THESIS

submitted to

Oregon State University

in partial fulfillment of
the requirements for the
degree of

Doctor of Philosophy

June 1971

APPROVED:

Redacted for Privacy

Professor of Chemical Engineering

in charge of major

Redacted for Privacy

Head of Department of Chemical Engineering

Redacted for Privacy

Dean of Graduate School

Date thesis is presented August 13, 1970

Typed by Clover Redfern for Leonard LeRoy Hovey

ACKNOWLEDGMENTS

The author wishes to express his sincere thanks and appreciation to the staff of the Chemical Engineering Department. Special thanks is extended to Dr. C. E. Wicks for his assistance and encouragement during the course of this program.

Financial support provided by the NDEA, the Chemical Engineering Department and Diamond Alkali is gratefully acknowledged and appreciated.

The assistance of Andre Caron, Joe Megy and Mike Franklin of the National Council for Stream Improvement has been most helpful.

The assistance of Billy Zumwalt and Ted Beckwith in the preparation of the figures is also acknowledged.

Also the sacrifices, encouragement and assistance of my wife and children is most greatly appreciated.

TABLE OF CONTENTS

LIST OF FIGURES

LIST OF TABLES

SURFACE RENEWAL RATE FOR THE ABSORPTION OF ODORIFEROUS SULFUR COMPOUNDS IN A WETTED WALL COLUMN

I. INTRODUCTION

In recent years there has developed considerable concern about the effects of air pollution. In the Pacific Northwest much of the public's concern is caused by the very noticeable, odoriferous, sulfur compounds emitted by the kraft process pulp mills. Although these compounds are small in quantity and emitted in low concentrations they are noticed because of low odor thresholds of detection. The odor threshold of detection for hydrogen sulfide has been reported as 0.8 parts per billion, that is 0.8 pounds hydrogen sulfide per billion pounds of air. For methyl mercaptan the odor threshold of detection has been reported as 2.1 parts per billion (23). Dimethyl sulfide has a reported odor threshold of detection of 1.0 part per billion. No odor threshold of detection has been reported for dimethyl disulfide but it is probably also in the parts per billion range.

Although hydrogen sulfide is reported as lethal at 500 parts per million (37), the other sulfur compounds present are much less toxic. Methyl mercaptan and dimethyl disulfide are reported to be fatal to rats in 15 minutes if at a concentration of 0.5 volume percent in air (25). Dimethyl sulfide is even less toxic, being fatal to rats in 15 minutes

if at a concentration of 5 volume percent in air (25). Studies carried out so far have failed to indicate that the odor components, at the low levels normally emitted by kraft pulp mills, increase the frequency of respiratory illnesses. Kraft odor emissions have neither been associated with adverse effects on plant growth nor with haze formation (37).

From the above it can be seen that the removal of the sulfides and mercaptan from kraft mill effluents is important only from an aesthetic point of view and not as a safety measure. Since the loss of sulfur from a typical kraft pulp mill is in the range of 1 to 20 pounds of reduced sulfur per ton of pulp, the recovery of sulfur cannot be justified on the basis of chemical makeup cost reduction; although this would help offset the recovery cost (37).

Source of the Problem

In the kraft pulping process hydrosulfide ion is one of the active pulping agents. Since the pulping process takes place in a water solution there will be an equilibrium between hydrosulfide ion and hydrogen sulfide; thus hydrogen sulfide is present as a component of the cooking liquor. A byproduct of the pulping reaction is the reaction with methoxylignin to give methyl mercaptan (29).

$$LigOMe + SH^- \rightarrow MeSH + LigO^- \qquad (1)$$

In an alkaline environment the methyl mercaptan reacts with caustic to given methyl sulfide ions (MeS^-). These methyl sulfide ions can react with methoxylignin to give dimethyl sulfide (29).

$$LigOMe + MeS^- \rightarrow Me_2S + LigO^- \qquad (2)$$

Dimethyl disulfide is formed by the oxidation of methyl mercaptan with air. This reaction takes place readily when the mercaptan is present as the sodium salt.

$$2MeSNa + \frac{1}{2} O_2 + H_2O \rightarrow MeSSMe + 2NaOH \qquad (3)$$

In the absence of air, the reaction of methyl mercaptan can take place in an alkaline environment to give dimethyl sulfide and hydrogen sulfide.

$$2MeSH \xrightarrow{OH^-} Me_2S + H_2S \qquad (4)$$

Since the reaction of hydrosulfide ion with methoxylignin (Equation 1) has an enthalpy of activation of only 11,300 calories per gram mole and the reaction of methyl sulfide ion with methoxylignin (Equation 2) has an enthalpy of activation of only 7,600 calories per gram mole, these reactions are both relatively insensitive to temperature change and hence can continue to occur while the black liquor is being evaporated unless the methyl sulfide ion and the hydrosulfide ion

concentrations are reduced early in the evaporator train (29). By using black liquor oxidation the sodium sulfide is oxidized to thiosulfate or sulfite and the mercaptan is oxidized to disulfide and further production of methyl mercaptan and dimethyl sulfide in the evaporator train is avoided.

By properly operating the recovery furnace, the formation of the odoriferous sulfur in the recovery furnace can be held to a low level.

According to the previous discussion, the formation of the odoriferous sulfur compounds can be limited to the digester and the black liquor oxidation vessel. It is possible to burn these odoriferous sulfur compounds to SO_2 but this is just converting the pollutant to a less obnoxious form and does nothing to decrease the pollution. This study will consider absorption as a means of reducing the pollutants emitted.

Previous Investigations

Absorption of Odoriferous Sulfur Compounds

A number of articles have been published about the absorption of hydrogen sulfide. Astarita and Gioia have published several articles (1, 2, 3, 13) about the absorption of hydrogen sulfide in a wetted wall column with an absorbing liquid which reacts with the hydrogen sulfide. These works have shown that hydrogen sulfide can be

selectively absorbed in the presence of carbon dioxide under controlled conditions.

Carter (8) has studied the effect of an oxidizing agent, sodium hypohalite, on the absorption of hydrogen sulfide into a laminar jet. The studies by Carter and also those by Astarita and Gioia, used pure hydrogen sulfide gas so that the gas phase resistance to mass transfer was negligible.

Oloman and coworkers (32) studied the use of a packed column for absorbing hydrogen sulfide with a sodium hydroxide solution from a kraft mill stack. The study indicated that about ninety percent removal of hydrogen sulfide could be obtained. However, for a 500 ton per day mill it would require a tower 20 feet in diameter with a packed height of 10 feet and 3000 gallons per minute of recycling carbonate liquor having a pH of about 9.5. The pH was found to be critical because too high pH gave excessive caustic consumption, due to the carbon dioxide absorption, and when the pH was too low the effect of the reacting liquid was lost, giving only physical absorption.

Jensen and coworkers (18) studied the absorption of dilute hydrogen sulfide and methyl mercaptan into sodium hydroxide and sodium hypohalite solutions. Their studies showed that the sodium hypohalite solution was not effective for methyl mercaptan absorption because the methyl mercaptan was converted to dimethyl disulfide and lost in the effluent gas. The study found that the gas absorption was

independent of liquid flow rate when the hydroxide to solute mole ratio was greater than 1.8.

Landry (21) also studied the absorption of methyl mercaptan in sodium hydroxide solution. His study used a laminar jet of sodium hydroxide for the absorbing fluid.

McCarthy and coworkers have published a series of articles (17, 27, 28) on steam stripping the volatile components from kraft mill condensates. The work was quite limited but did give some equilibrium values.

Several researchers have reported using various heavy metal chlorides for the removal of dimethyl sulfide. Brown and Wheeler (7) reported mercuric chloride gave quantitative removal of the dimethyl sulfide from the reaction mixture of 2-pentyl iodide and sodium methyl mercaptide. Bassette and Whitnah (5) reported that treatment of an aqueous solution of low molecular weight carbonyl compounds, 2-propanol, and dimethyl sulfide gave virtually complete elimination of dimethyl sulfide and had no effect on the other compounds. Phillips (34) studied the effect of dimethyl sulfide on solutions of several heavy metal chlorides. He found that all the chlorides studied, including mercuric and cupric, gave precipitates when treated with dimethyl sulfide. The precipitates formed could be decomposed by heating to temperatures in the range of 100 to 200°C (centigrade).

Related Absorption Studies

Scriven and Pigford (38) studied the absorption of carbon dioxide in short laminar water jets and found that equilibrium prevails at the interface. Lynn and coworkers (26) found that for the absorption of sulfur dioxide in a short wetted wall column the interface was at equilibrium.

Lynn and coworkers (26) and Nijsing and coworkers (20) have studied the entrance effects in wetted wall columns. Lynn studied the absorption of sulfur dioxide in water which formed an external film on a pipe 1 1/2-centimeters in diameter with exposed lengths varied between one and five centimeters. Nijsing studied the absorption of carbon dioxide into water and sodium hydroxide solutions. He used an internally wetted column 2.86 centimeters in diameter with exposed lengths of from 2 to 26 centimeters. Both of these workers concluded that entrance effects were negligible after the liquid had flowed a distance of 20 times the film thickness.

Several studies have been published relative to the effects of gas flow rate on gas phase mass transfer. Reker and coworkers (36) reported that for the vaporization of methanol and carbon tetrachloride into an air stream, the gas phase mass transfer coefficient was proportional to the Reynolds number to the 0.83 power. He studied a Reynolds number range of 2500 to 6000. Sharma and Vidwans (39) studied the absorption of sulfur dioxide, chlorine, ammonia and several other

gases in various liquid solutions in a packed column. They found that for gas velocity over about a three fold range, the gas phase mass transfer coefficient was proportional to gas Reynolds number to a power between 0.6 and 0.85.

Mehta and Sharma (31) studied the effect of diffusivity and Schmidt number on the gas phase mass transfer coefficients in a bubble column. They found that with a 14-fold variation in diffusivity and a 5-fold variation in Schmidt number the gas phase mass transfer coefficient was proportional to the square root of diffusivity. In this study they found the gas phase mass transfer coefficient was proportional to velocity to the 0.75 power.

Banerjee and coworkers (4) correlated the liquid phase mass transfer coefficient to the flow properties of the system and an eddy length scale to arrive at an equation for mass transfer coefficients in terms of viscous dissipation of energy. Using empirical relationships for wave characteristics, he found that the mass transfer coefficients could be expressed as

$$k_L = 2.93 \times 10^{-3} D_L^{1/2} N_{ReL}^{0.933} \qquad (5)$$

where the constant 2.93×10^{-3} includes the term $\nu^{1/6}$.

Banerjee presented data for absorption of oxygen and carbon dioxide in water from the works of Emmert and Pigford, Kamei and

Oishi, and Miller. These works represent the use of internally wetted wall columns with lengths of from 2.4 to 8.2 feet. The column diameters were from 0.99 inch to 1.89 inches. The temperature range covered was from 8.5 to 50°C. The data presented ranged from a liquid Reynolds number of 1500 to 8500. Although the data presented agreed with the equation presented, there is apparent deviation of the data from the equation at both ends of the Reynolds number range.

Equilibrium Studies

Vapor-liquid equilibrium data for methyl mercaptan have been reported in the literature by several authors.

Reid (35) reported a solubility of 23.3 grams methyl mercaptan per liter of water. The value was given in a table with no reference to the original work. Neither the temperature at which the data were taken nor the method used to collect the data were given. However, if a temperature of 25°C were assumed, Henry's law constant would be 0.0842, based on expressing concentration in both liquid and gas phase in pound moles per cubic foot.

Shih and coworkers (40) gave some data for the partial pressure of methyl mercaptan over liquid solutions with fixed methyl mercaptan concentrations when the liquid solutions varied from pH 7 to 14. For a pH of 7 or 8 and a 0.01 N (normal) methyl mercaptan solution the following equation was given:

$$\log_{10} P = 4.0704 - \frac{989.4}{T} \qquad (6)$$

(A table of nomenclature and units of measurement is given in Appendix F.) This study indicated that up to 0.04 N methyl mercaptan concentration in the liquid, the partial pressure was proportional to the concentration. The data presented gave an estimated accuracy of plus or minus 15% and were taken over the temperature range of 80°C to 185°C. If the assumption were made that the data could be extrapolated to 25°C then a Henry's law constant of 0.0284 would be obtained.

Maahs and coworkers (27) have reported equilibrium values for methyl mercaptan in water solution for the temperature range of 3°C to 68°C. Nine data points, with about a 25% difference on duplicate points, were given. A Henry's law constant at 25°C of 0.100 was obtained using this reference.

Landry (21) reported a solubility of methyl mercaptan in water at 25°C and one atmosphere methyl mercaptan pressure as 2.45×10^{-4} gram moles per milliliter. A Henry's law constant of 0.167 was obtained from this value.

The most extensive data found for methyl mercaptan in water were presented by Harkness and Kelman (15). Their results were presented in graphical form with the slope of the least-squares-fit straight line through the data given. The equation for the Bunsen coefficient was found to be:

$$\log_{10}\alpha = \frac{1352.1}{T} - 3.757 \qquad (7)$$

The partial pressure of methyl mercaptan from 30 mm (millimeters mercury) to 700 mm was studied and the concentration in the liquid was found to be proportional to the partial pressure of methyl mercaptan. A Henry's law constant at 25°C of 0.152 was calculated from this data. This data showed a range of plus or minus 0.1 for $\log_{10}\alpha$ and, in the range of 25°C, most of the data fell on the low side; this would give lower values of α but higher values of the Henry's law constant.

Figure 1 shows a plot of the Henry's law constants versus temperature for methyl mercaptan. The value used in the present work is shown as the solid line. This is based on the data reported by Landry and the temperature dependence reported by Harkness and Kelman. The data of Shih and also Maahs was not considered reliable. In addition to the extrapolation and inaccuracy mentioned earlier, both were done in the same laboratory and no discussion of the inconsistencies between the two sets was given.

The only published values of equilibrium data for dimethyl sulfide and dimethyl disulfide which could be found were those of Maahs and coworkers (27). Henry's law constants at 25°C of 0.0239 and 0.0178 for dimethyl sulfide and dimethyl disulfide, respectively, were calculated from these data. A check on the Henry's law constant,

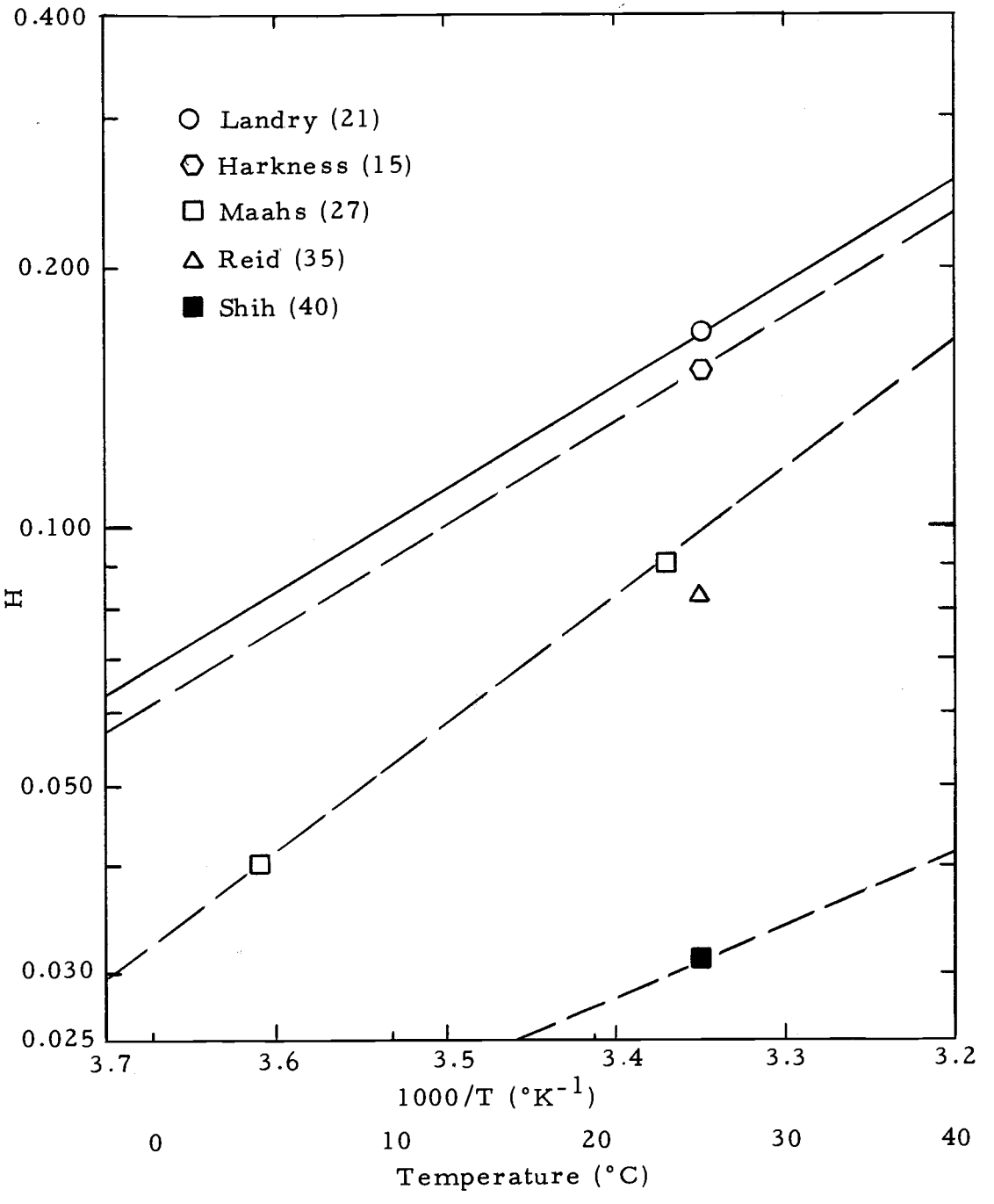

Figure 1. Henry's law constant for methyl mercaptan in water at various temperatures.

using the solubility reported and the partial pressures of the sulfides calculated from the data given by White and coworkers (43) was made. By this method Henry's law constants of 0.314 and 0.0497 for dimethyl sulfide and dimethyl disulfide, respectively, were calculated. Because of the above discrepancies and the discrepancies in their methyl mercaptan data, their equilibrium data for the dimethyl sulfide-water and the dimethyl disulfide-water systems were not used. Dimethyl sulfide-water and dimethyl disulfide-water equilibrium data used in this study were based on analyses performed by the National Council for Stream Improvement for the author. Calculations of these values are shown in Appendix A.

In view of the limited amount of work available on the removal of sulfide gases, this work was undertaken. The object of this work was to obtain information on both the gas-side and the liquid-side mass transfer coefficients for the removal of sulfide gases from streams with low sulfide concentrations.

II. THEORETICAL BACKGROUND

One of the methods available to reduce the levels of pollution is to absorb the offending material and then recover it from the absorbing liquid. In an absorption process there are two principle resistances that impede absorption. The gas-side resistance is the resistance to the migration of the molecules being absorbed to the gas-liquid interface. The liquid-side resistance is the resistance to the migration of the absorbed molecules away from the gas-liquid interface. Frequently one or the other of these two resistances is negligible compared to the other. For example, if a pure gas or a sparingly soluble dilute gas is being absorbed the liquid-side resistance is the major part of the resistance to the mass transfer operation. Conversely for a very soluble dilute gas, often the gas-side resistance is the major resistance to the mass transfer operation. For the systems used in this investigation, the liquid and gas-side resistances are about equally important in the absence of reaction in liquid.

In order for design data to be useful in any system other than the particular system from which it was taken, it is desirable to develop a mathematical model which uses the important physical variables involved in the operation to describe the transport mechanism of the system. If the model is valid then by knowing the important physical variables for a second system the data can be used for the design of

the second system.

Two Film Model

There are two major models which have been proposed and are currently used for the interpretation of absorption data. The two-film theory was proposed by Whitman in 1923 (44). This model relies on the following series of assumptions:

1. Steady state conditions exist in both phases.
2. The rate of transfer is proportional to the concentration gradient.
3. Equilibrium exists between the liquid and the vapor at the interface with no interfacial resistance to flow.
4. Hold up at the interface is negligible.

This model and these assumptions lead to the following equations for mass flux:

$$N_A = K_{CG}(C_G - C_G^*) \tag{8}$$

$$N_A = K_L(C_L^* - C_L) \tag{9}$$

$$N_A = k_{CG}(C_G - C_{Gi}) \tag{10}$$

$$N_A = k_L(C_{Li} - C_L) \tag{11}$$

These equations are interrelated for the case of a dilute gas obeying Henry's law by the following relationships:

$$\frac{1}{K_{CG}} = \frac{1}{k_{CG}} + \frac{H}{k_L} \tag{12}$$

$$\frac{1}{K_L} = \frac{1}{Hk_{CG}} + \frac{1}{k_L} \tag{13}$$

The development of these equations is shown in Appendix B.

From Fick's first law the equation for mass flux is:

$$\vec{N}_A = X_A(\vec{N}_A + \vec{N}_B) - CD_{AB}\nabla X_A \tag{14}$$

For the special case of equimolar counter diffusion and where only diffusion in one direction is important this reduces to:

$$N_A = - D_{AB} \frac{dC_A}{dx} \tag{15}$$

This form can be used for flow down a cylinder if the curvature is negligible compared to the thickness of the film, which is the case in the present work. For the Whitman two film model no material is accumulated in the film so

$$\frac{\partial N_A}{\partial x} = 0 \tag{16}$$

Applying this condition to Equation 15 gives Fick's second law for steady state.

$$\frac{\partial^2 C_A}{\partial x^2} = 0 \tag{17}$$

B. C. 1) $x = 0 \qquad C_A = C_{Ai}$

2) $x = \delta \qquad C_A = C_A^{\infty}$

The solution for this equation is

$$C_A = c_1 x + c_2 \tag{18}$$

which upon substituting boundary conditions gives

$$C_A = \frac{(C_A^{\infty} - C_{Ai})x}{\delta} + C_{Ai} \tag{19}$$

Combining Equations 15 and 19 gives:

$$N_A = \frac{D_{AB}}{\delta} (C_{Ai} - C_A^{\infty}) \tag{20}$$

This is the same form as Equation 11 where

$$k_L = \frac{D_{AB}}{\delta} \tag{21}$$

It should be noted that Equation 15 was set up so that mass transfer was in the direction of increasing distance from the interface. Since for the gas phase, the transfer is in the opposite direction, i.e., out

of the gas phase, Equation 20 is the same form as Equation 10 where

$$k_{CG} = \frac{D_{AB}}{\delta} \tag{22}$$

Penetration Models

A second model is the penetration model which was proposed by Higbie in 1935 (16). This model relies on the following assumptions:

1. The rate of transfer is proportional to the concentration gradient.
2. Equilibrium exists between the liquid and the vapor at the interface with no interfacial resistance to the mass transfer.

Higbie also assumed the contact time at the interface was a constant value for all the material and the interfacial film had an infinite depth. This model was modified by Danckwerts in 1951 (10) to introduce a random time of contact at the interface for the elements of flow. This model was further modified by W. E. Dobbins in 1955 (30) to include a finite thickness, δ, for the region of resistance to mass transfer. The concentration at the boundary of the region of resistance to mass transfer was taken as the bulk stream concentration. All three of these modifications give flux and resistance equations of the same form as Equations 8, 9, 10, 11 and 12.

For the penetration models, Equation 15 still applies except

that in this model material can accumulate in the film so that Equation 16 is now:

$$\frac{\partial N_A}{\partial x} = - \frac{\partial C_A}{\partial t} \tag{23}$$

Equations 15 and 23 can now be combined to give Fick's second law of diffusion for the unsteady state case

$$\frac{\partial C_A}{\partial t} = D_{AB} \frac{\partial^2 C_A}{\partial x^2} \tag{24}$$

B. C. 1) $t = 0 \quad C_A = C_A^\infty \quad x > 0$

2) $t > 0 \quad C_A = C_{Ai} \quad x = 0$

3) $t > 0 \quad C_A = C_A^\infty \quad x = \infty$

Equation 24 is readily solved by making a change of variable to

$$y_A = \frac{C_A - C_A^\infty}{C_{Ai} - C_A^\infty} \tag{25}$$

giving

$$\frac{\partial y_A}{\partial t} = D_{AB} \frac{\partial^2 y_A}{\partial x^2} \tag{26}$$

B. C. 1) $t = 0 \quad x > 0 \quad y_A = 0$

2) $t > 0 \quad x = 0 \quad y_A = 1$

3) $t > 0 \quad x = \infty \quad y_A = 0$

When the Laplace transform of Equation 26 with respect to t is taken, the following equation is obtained.

$$\frac{\partial^2 \bar{y}_A}{\partial x^2} - \frac{s}{D_{AB}} \bar{y}_A = 0 \tag{27}$$

B. C. 1) $x = 0 \quad \bar{y}_A = 1/s$

2) $x = \infty \quad \bar{y}_A = 0$

Equation 27 is solved to get

$$\bar{y}_A = c_1 e^{-\sqrt{s/D_{AB}}\,x} + c_2 e^{+\sqrt{s/D_{AB}}\,x} \tag{28}$$

which upon applying the boundary conditions gives

$$\bar{y}_A = (1/s) e^{-x\sqrt{s/D_{AB}}} \tag{29}$$

When the inverse transformation of Equation 29 is taken the following solution for Equation 26 is obtained.

$$y_A = \operatorname{erfc} \frac{x}{\sqrt{4D_{AB}t}} \tag{30}$$

which gives the solution to Equation 24 as

$$C_A = C_A^{\infty} + (C_{Ai} - C_A^{\infty}) \operatorname{erfc} \frac{x}{\sqrt{4tD_{AB}}} \tag{31}$$

The mass flux can be found by evaluating Equation 15 at the gas-liquid interface where x is 0,

$$\frac{\partial C_A}{\partial x} = - \frac{(C_{Ai} - C_A^{\infty})}{\sqrt{\pi t D_{AB}}} e^{-x^2/(4tD_{AB})} \tag{32}$$

which at the interface is

$$\left.\frac{\partial C_A}{\partial x}\right|_{x=0} = - \frac{(C_{Ai} - C_A^{\infty})}{\sqrt{\pi t D_{AB}}} \tag{33}$$

The Higbie model assumes the exposure times of all elements are constant equal to t_e; this gives

$$N_A = \sqrt{\frac{D_{AB}}{\pi t_e}} (C_{Ai} - C_A^{\infty}) \tag{34}$$

Equation 34 is the same form as Equation 10 or 11, so

$$k_L = \sqrt{\frac{D_{AB}}{\pi t_e}} \tag{35}$$

and

$$k_{CG} = \sqrt{\frac{D_{AB}}{\pi t_e}} \tag{36}$$

for the liquid and gas phases, respectively.

For the Danckwerts model it is necessary to sum the mass flux for all elements since the age of the elements can differ. This gives

$$N_A = \int_0^\infty \varphi \left[-D_{AB} \left. \frac{\partial C_A}{\partial t} \right|_{x=0} \right] dt \tag{37}$$

where φ is the fraction of elements with age t.

The equation for φ is of the form

$$\varphi = se^{-st} \tag{38}$$

See Appendix C for the development of the equation for φ. Substituting Equation 38 into Equation 37 gives

$$N_A = -D_{AB} s \left[\int_0^\infty e^{-st} \left. \frac{\partial C_A}{\partial x} \right|_{x=0} dt \right] \tag{39}$$

Comparing the terms in the brackets in Equation 39 to the definition of the Laplace transform

$$\left. \frac{d\bar{C}_A}{dx} \right|_{x=0} = \int_0^\infty e^{-st} \left. \frac{\partial C_A}{\partial x} \right|_{x=0} dt \tag{40}$$

shows

$$N_A = -D_{AB} s \left. \frac{d\bar{C}_A}{dx} \right|_{x=0} \tag{41}$$

Evaluation of either Equation 37 or Equation 41 gives

$$N_A = \sqrt{D_{AB} s} \, (C_{Ai} - C_A^\infty) \tag{42}$$

where Equation 42 is the same form as Equations 10 and 11, with

$$k_L = \sqrt{D_{AB} s} \tag{43}$$

and

$$k_{CG} = \sqrt{D_{AB} s} \tag{44}$$

for the liquid and gas phases, respectively.

The modification proposed by Dobbins changes the third boundary condition of Equation 24 to give

$$\frac{\partial C_A}{\partial t} = D_{AB} \frac{\partial^2 C_A}{\partial x^2} \tag{45}$$

B. C. 1) $t = 0 \quad x > 0 \quad C_A = C_A^\infty$

2) $t > 0 \quad x = 0 \quad C_A = C_{Ai}$

3) $t > 0 \quad x = \delta \quad C_A = C_A^\infty$

The following equation is obtained after making the same change of variable as before and taking the Laplace transform.

$$\frac{\partial^2 \bar{y}_A}{\partial x^2} - \frac{s}{D_{AB}} \bar{y}_A = 0 \tag{46}$$

B. C. 1) $x = 0 \quad \bar{y}_A = 1/s$

2) $x = \delta \quad \bar{y}_A = 0$

The solution to this equation can be written as

$$\bar{y}_A = c_1 \sinh\left[x\sqrt{\frac{s}{D_{AB}}}\right] + c_2 \cosh\left[x\sqrt{\frac{s}{D_{AB}}}\right] \tag{47}$$

Using the boundary conditions one finds

$$\bar{y}_A = \frac{1}{s}\cosh\left[x\sqrt{\frac{s}{D_{AB}}}\right] - \frac{1}{s}\coth\left[\delta\sqrt{\frac{s}{D_{AB}}}\right]\sinh\left[x\sqrt{\frac{s}{D_{AB}}}\right] \tag{48}$$

This gives

$$\left.\frac{d\bar{y}_A}{dx}\right|_{x=0} = \frac{-1}{\sqrt{D_{AB}s}}\coth\left[\delta\sqrt{\frac{s}{D_{AB}}}\right] \tag{49}$$

Combining Equations 41, 49 and 25 gives

$$N_A = \sqrt{D_{AB}s}\coth\left[\delta\sqrt{\frac{s}{D_{AB}}}\right]\left[C_{Ai}-C_A^{\infty}\right] \tag{50}$$

which is also of the same form as Equation 10 and 11 where

$$k_L = \sqrt{D_{AB}s}\coth\left[\delta\sqrt{\frac{s}{D_{AB}}}\right] \tag{51}$$

and

$$k_{CG} = \sqrt{D_{AB}s}\coth\left[\delta\sqrt{\frac{s}{D_{AB}}}\right] \tag{52}$$

for the liquid and gas phases, respectively.

An interesting feature of the Dobbins model is that when $(\delta\sqrt{s/D_{AB}})$, is small, i.e., less than 0.2,

$$\coth\left[\delta\sqrt{\frac{s}{D_{AB}}}\right] \cong \sqrt{\frac{D_{AB}}{\delta^2 s}} \tag{53}$$

so

$$k_L = \frac{D_{AB}}{\delta} \tag{21}$$

and

$$k_{CG} = \frac{D_{AB}}{\delta} \tag{22}$$

the same as for the two film model. When $\delta\sqrt{(s/D_{AB})}$ is larger than 5

$$\coth\left[\delta\sqrt{\frac{s}{D_{AB}}}\right] = 1 \tag{54}$$

so

$$k_L = \sqrt{D_{AB}s} \tag{43}$$

and

$$k_{CG} = \sqrt{D_{AB}s} \tag{44}$$

which are the relationships desired for the penetration model.

Calculation of Mass Transfer Coefficients

For the overall transfer coefficient calculation the development will be considered on the same basis as that normally used for a packed tower. See Figure 2 for a sketch of the tower and the nomenclature used in this development. The assumption will be made that

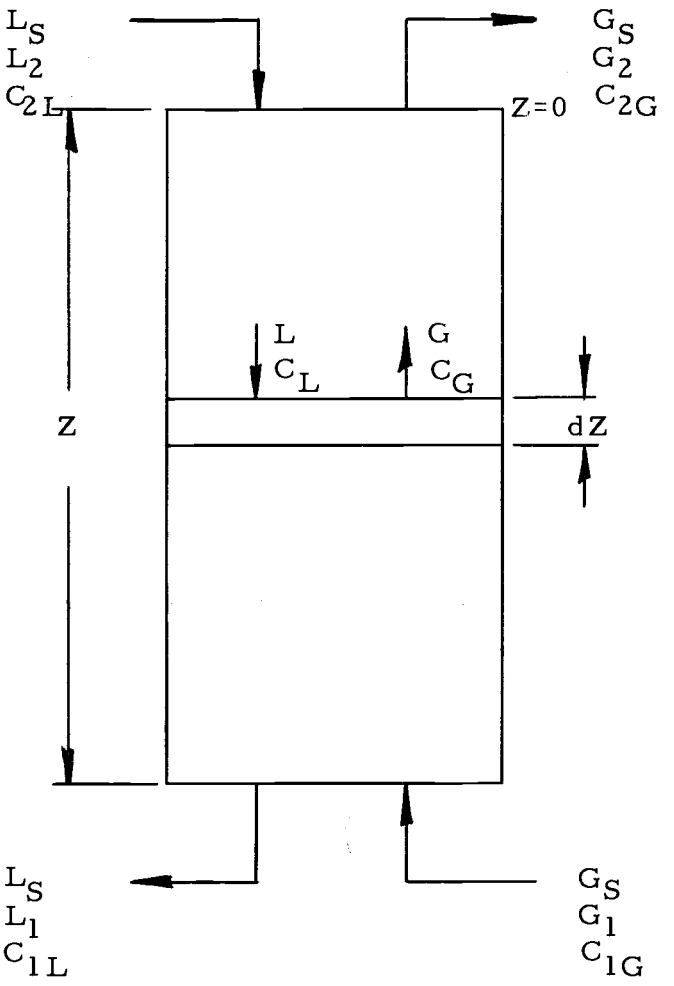

Figure 2. Flow quantities for absorption tower.

in the dilute liquid concentrations encountered in this investigation the equilibrium-solubility curve is straight over the concentration range considered. By making a material balance on the differential height (dZ) of the column, it is found that:

$$d(GC_G) = K_{CG}(C_G - C_G^*)adZ \tag{55}$$

This is saying that the change in solute in the gas phase is equal to the amount of material crossing the gas-liquid interface. Both G, the gas velocity, and C_G, the gas composition, vary from one end of the tower to the other. However, for dilute gases such as those used in the experimental work, the variation in gas velocity can be neglected, giving

$$Gd(C_G) = K_{CG}(C_G - C_G^*)adZ \tag{56}$$

Equation 56 can be rearranged to give

$$\frac{d(C_G)}{(C_G - C_G^*)} = \frac{K_{CG}}{G}\, adZ \tag{57}$$

The left hand side of Equation 57 in integrated form is commonly referred to as the number of transfer units and the right hand side of the equation is referred to as the height of column multiplied by one over the height per transfer unit.

$$N'_{tOG} = \int_{C_{G2}}^{C_{G1}} \frac{d(C_G)}{(C_G - C_G^*)} \tag{58}$$

$$H'_{tOG} = \frac{G}{K_{CG}a} \tag{59}$$

$$Z = (H'_{tOG})(N'_{tOG}) \tag{60}$$

For the case where the gas obeys Henry's law

$$C_G^* = HC_L \tag{61}$$

Since the solutions are both dilute, liquid flow rate will also be essentially constant so a material balance around a section of the column is,

$$(C_G - C_{G2})Q_G = Q_L(C_L - C_{L2}) \tag{62}$$

where

$$Q_G = (G)(A_C) \tag{63}$$

and

$$Q_L = (L)(A_C) \tag{64}$$

Equation 62 may be rearranged to give

$$C_L = \frac{Q_G}{Q_L}(C_G - C_{G2}) + C_{L2} \tag{65}$$

Combining Equations 61 and 65 gives,

$$C_G^* = \frac{HQ_G}{Q_L}(C_G - C_{G2}) + C_{L2} \tag{66}$$

Equation 66 can now be substituted into Equation 58 giving,

$$N'_{tOG} = \int_{C_{G2}}^{C_{G1}} \frac{dC_G}{C_G(1 - \frac{HQ_G}{Q_L}) + \frac{HQ_G}{Q_L} C_{G2} - C_{L2}} \tag{67}$$

Equation 67 is integrated after noting C_{L2} is zero in this experimental work to give,

$$N'_{tOG} = \frac{1}{(1 - \frac{HQ_G}{Q_L})} \ln \left[\frac{\frac{HQ_G}{Q_L}(C_{G2} - C_{G1}) + C_{G1}}{C_{G2}} \right] \tag{68}$$

Equations 59 and 60 can be combined to give,

$$K_{CG} = \frac{(N'_{tOG})(G)}{(a)(Z)} \tag{69}$$

For the case of sulfur dioxide absorption the gas phase composition is constant so that it is better to write Equation 55 as

$$d(LC_L) = K_L(C_L^* - C_L)adZ \tag{70}$$

which can be rearranged to give

$$\frac{dC_L}{(C_L^* - C_L)} = \frac{K_L a}{L} dZ \tag{71}$$

The height per transfer unit is now,

$$N'_{tOL} = \int_{C_{L2}}^{C_{L1}} \frac{dC_L}{C_L^* - C_L} \tag{72}$$

Since a pure gas phase in involved C_L^* is a constant, the saturation value. Equation 72 can be integrated to give

$$N'_{tOL} = - \ln\left[\frac{C_L^* - C_{L1}}{C_L^* - C_{L2}}\right] = \ln\left[\frac{C_L^* - C_{L2}}{C_L^* - C_{L1}}\right] \tag{73}$$

Equation 73 and 71 can be combined to give

$$K_L = \frac{(N'_{tOL})(L)}{(a)(Z)} \tag{74}$$

Examination of Equations 68 and 69 readily reveals that only the ratio of the inlet and outlet concentrations are important and not the absolute value. This means that the factor to convert area under the chromatograph peak to concentration is not important in obtaining the correct value of overall transfer coefficient.

To obtain the individual film transfer coefficients, the additive resistance feature is noted

$$\frac{1}{K_{CG}} = \frac{1}{k_{CG}} + \frac{H}{k_L} \tag{12}$$

$$\frac{1}{K_L} = \frac{1}{k_L} + \frac{1}{Hk_{CG}} \tag{13}$$

For the absorption of sulfur dioxide in water pure sulfur dioxide gas was used hence there was no gas phase resistance because the interface gas composition is the same as the bulk composition; the overall transfer coefficient is then equal to the liquid film transfer coefficient. For the absorption of the sulfides and mercaptan into water, it was necessary to separate the two film coefficients. This was done by absorbing methyl mercaptan in sodium hydroxide solution in which the liquid film resistance is negligible. The data confirmed that only the gas phase resistance was important since liquid flow rate had no effect on the overall mass transfer coefficient. The gas-side transfer coefficient was then expressed as a function of the gas Reynolds number. The gas-side transfer coefficient was also used in the calculation of the liquid film coefficient when the absorbing medium was water. For the sulfides the gas transfer coefficient was adjusted, as suggested by the penetration model, by ratioing the reciprocal of the square root of diffusivity as follows:

$$(k_{CG})_{sulfide} = (k_{CG})_{mercaptan} \sqrt{\frac{D_{sulfide\text{-}air}}{D_{mercaptan\text{-}air}}} \tag{75}$$

A reacting liquid was used to make the liquid phase resistance negligible compared to the gas phase resistance. Mercuric chloride was found to be a suitable reacting liquid for dimethyl sulfide and it was used to check the applicability of the penetration model. Since no reacting liquid could be found for the dimethyl disulfide, it was necessary to rely on the penetration model exclusively for this component.

Calculation of Reynolds Numbers

The liquid phase Reynolds number was

$$N_{Re} = \frac{4\Gamma}{\mu} \tag{76}$$

where Γ can be written as

$$\Gamma = \frac{Q_L \rho}{W} = \frac{\delta'^3 \rho g}{3\nu} \tag{77}$$

δ' is the film thickness and W is the wetted perimeter.

$$W = \pi(d_c + 2\delta') \tag{78}$$

Accordingly,

$$\frac{Q_L \rho}{\pi(d_c + 2\delta')} = \frac{\delta'^3 \rho g}{3\nu} \tag{79}$$

As a first approximation δ' can be neglected in the $(d_c + 2\delta')$ term since it is small compared to the pipe radius. (This approximation

introduces an error of 2 to 5 percent.) With this approximation Equation 79 can be rearranged to

$$Q_L \cong \frac{\pi d_c g}{3\nu} \delta'^3 \tag{80}$$

All of the terms in this equation are known except δ', so δ' can be found. By using this first approximation value of δ' to obtain $(d_c+2\delta')$, Equation 79 can be solved for δ' with an error of less than 1 percent.

$$\delta' = \left[\frac{3Q_L\nu}{\pi g[d_c+2(\frac{3Q_L\nu}{\pi g d_c})^{1/3}]} \right]^{1/3} \tag{81}$$

This value of δ' can then be used to solve for the liquid Reynolds number.

$$N_{Re} = \frac{4Q_L\rho}{W\mu} = \frac{4Q_L}{\nu(d_c+2\delta')} \tag{82}$$

The gas phase Reynolds number for flow in an annulus is based on the definition given in Knudsen and Katz (19).

$$N_{Re} = 2\frac{U}{\nu}\left(\frac{r_2^2 - r_{max}^2}{r_2}\right) \tag{83}$$

where

$$r_{max}^2 = \frac{r_2^2 - r_1^2}{2 \ln (r_2/r_1)} \tag{84}$$

These two equations are combined to give

$$N_{Re} = \frac{U[r_1^2 + r_2^2 (2 \ln (r_2/r_1) - 1)]}{\nu r_2 \ln (r_2/r_1)} \tag{85}$$

where r_1 is the liquid-gas interface radius and r_2 is the outside wall radius of the gas chamber. The average velocity (U) is

$$U = \frac{Q_G}{\pi (r_2^2 - (d_c/2 + \delta')^2)} \tag{86}$$

III. DESCRIPTION OF EQUIPMENT AND CHEMICALS

The absorption investigations were made in a falling-film tower in which the liquid flowed down the outside of an inner pipe countercurrent to the gas flow. Liquid flow rates were controlled by maintaining a constant head across a restriction in the inlet liquid line. Gas flow rates were controlled by having a constant displacement liquid flow into the gas feed tank; the displacement liquid flow rate was controlled by maintaining a constant head across a restriction in its inlet line. The displacement liquid was saturated with the specific sulfur compound being absorbed at the partial pressure of this compound in the feed gas. Since the displacement liquid was in equilibrium with the feed gas, the gas going to the tower, a constant feed gas composition was maintained. Figure 3 shows a sketch of the flow system used.

Tower

The absorption tower, which is shown as item C in Figure 3 was constructed of plexiglass and type 316 stainless steel. The wetted wall was formed on the outside of a schedule 40, 1/4-inch stainless steel pipe which was machined to an outside diameter of 1/2-inch and had a length of 18 inches. The base assembly of the tower is shown in Figure 4. The bottom of the column extended about 1/8-inch below

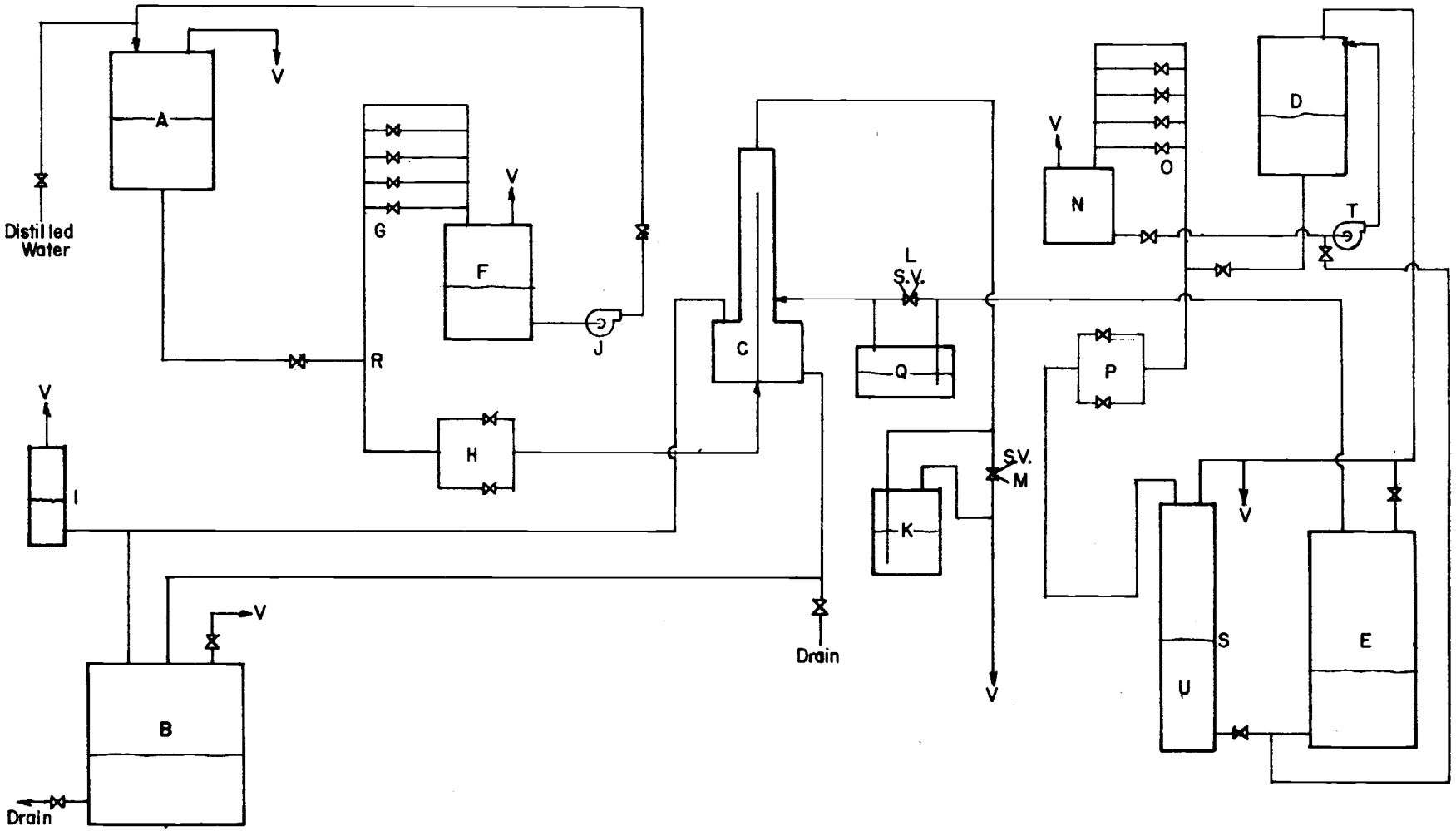

FLOW DIAGRAM

Figure 3. Flow diagram.

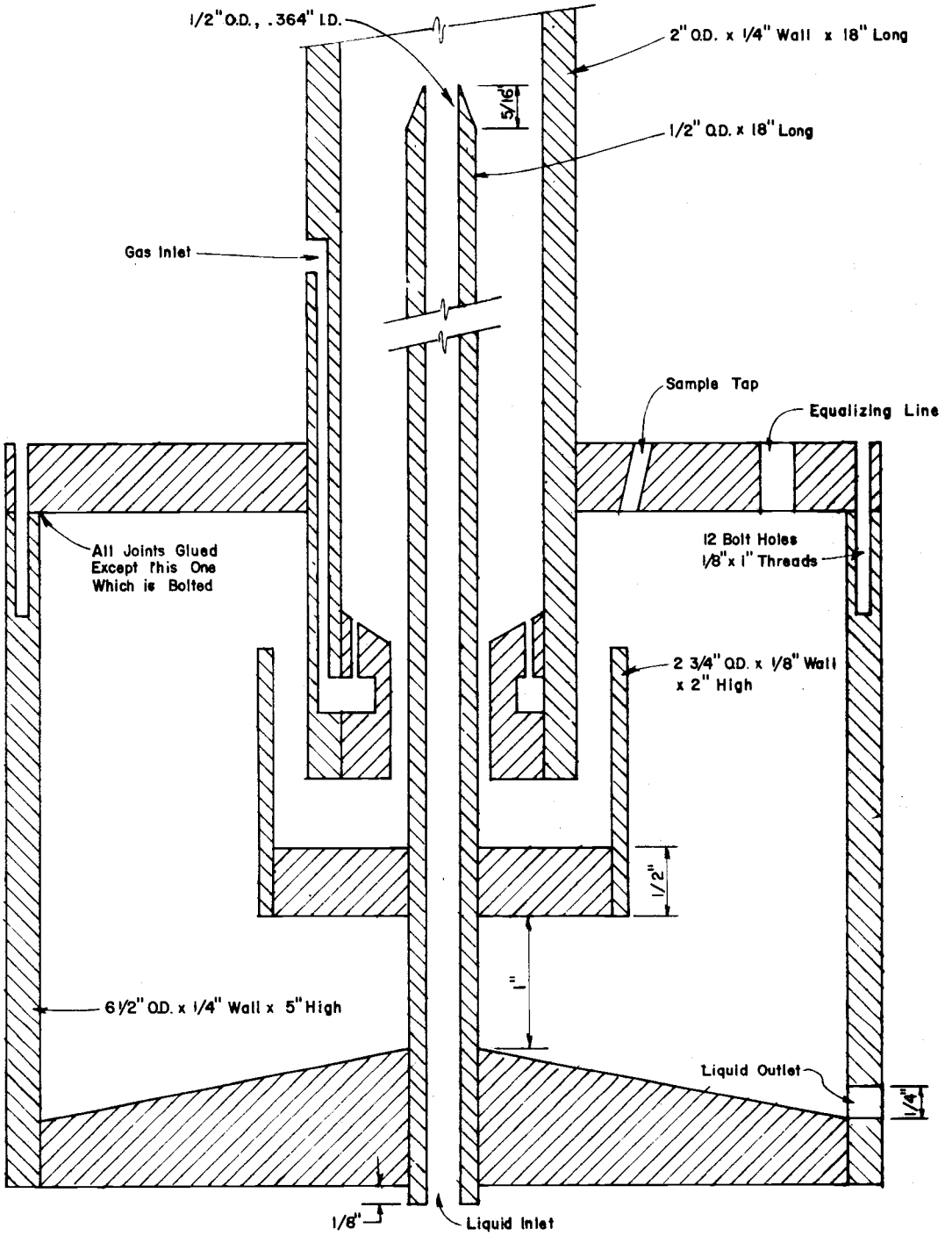

Figure 4. Tower base assembly.

the baseplate so that about 13 7/8-inches of wetted length were in contact with the gas. The top of the column was machined to a knife edge with the high point in the center and tapered down 5/16-inch from the top on the outside.

The top of the base reservoir was bolted onto the walls of the base assembly with a 1/32-inch gasket between the two surfaces. The remainder of the tower was constructed from plexiglass with the joints all solvent welded. The liquid seal box was held in place by 4 support rods from the baseplate to maintain the liquid seal box 1 inch from the base at the center.

The gas was distributed around the column by eight openings, 1/8-inch in diameter, in the bottom gas distributor. See Figure 5 for details of the gas distributor construction. Figure 6 shows the details of construction of the gas chamber. The gas entered an opening in the outside wall and flowed down through the wall to the bottom distributor. The gas chamber was 1 1/2-inches in inside diameter with an open length of approximately 16 inches.

Storage Vessels

The absorbing liquid storage reservoir, which is item A in Figure 3, was a 13 gallon, Nalgene, polyethylene carboy with a bottom outlet serrated nipple. The top was closed with a two-hole, number 13 1/2 rubber stopper, through which passed two glass nipples, three

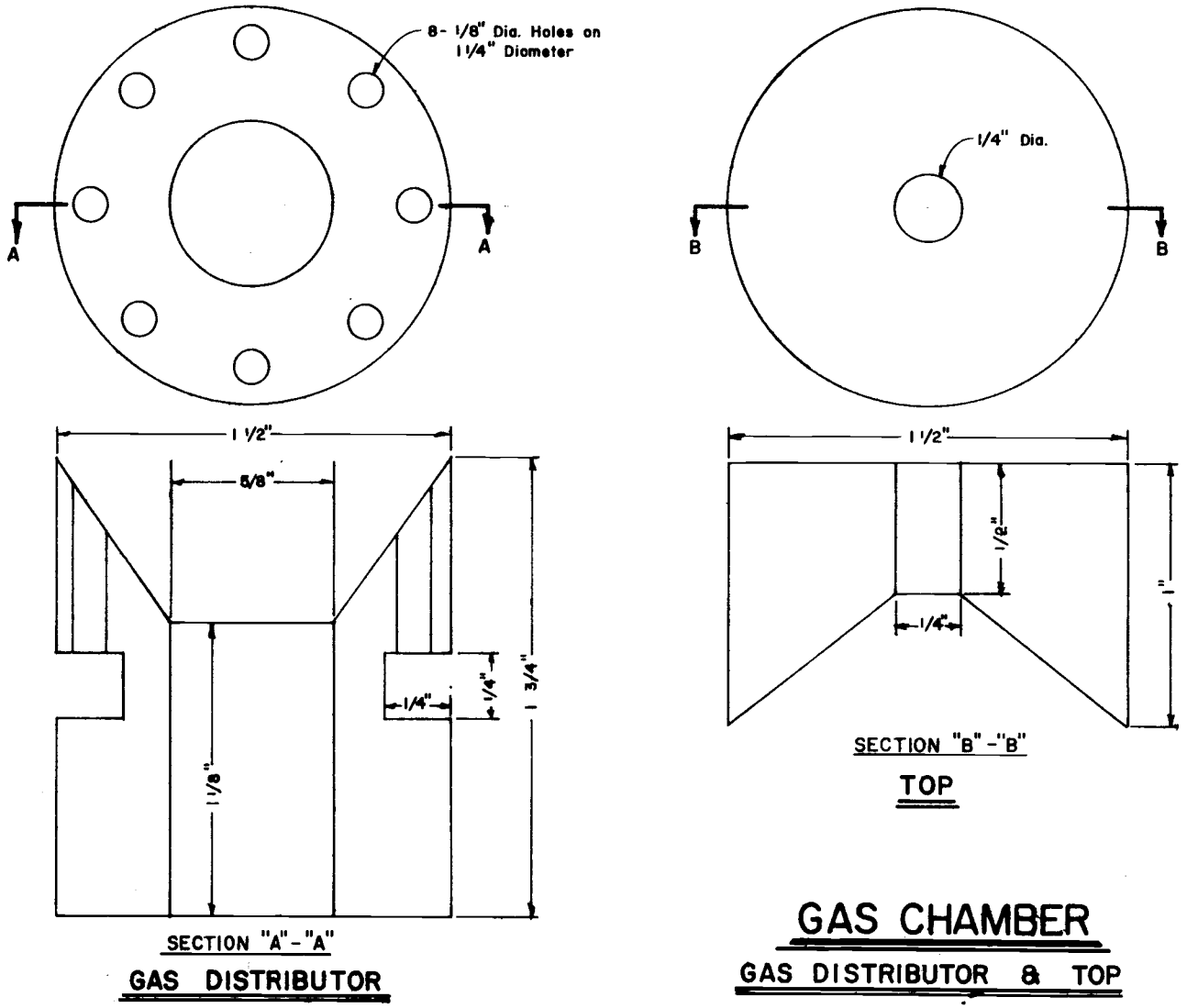

Figure 5. Gas distributor and gas outlet.

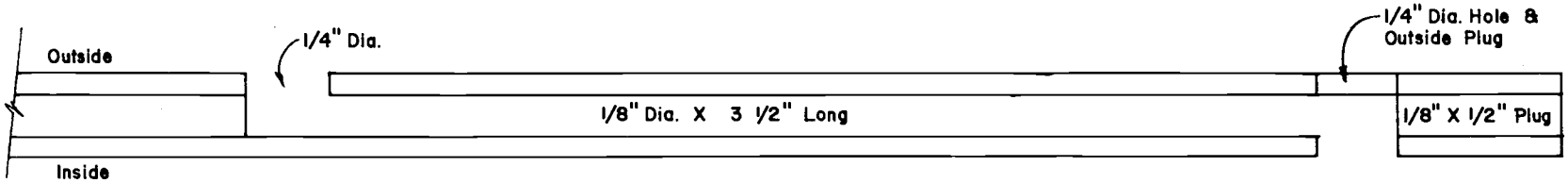

GAS INLET SECTION

Scale: 1" = 1/2"

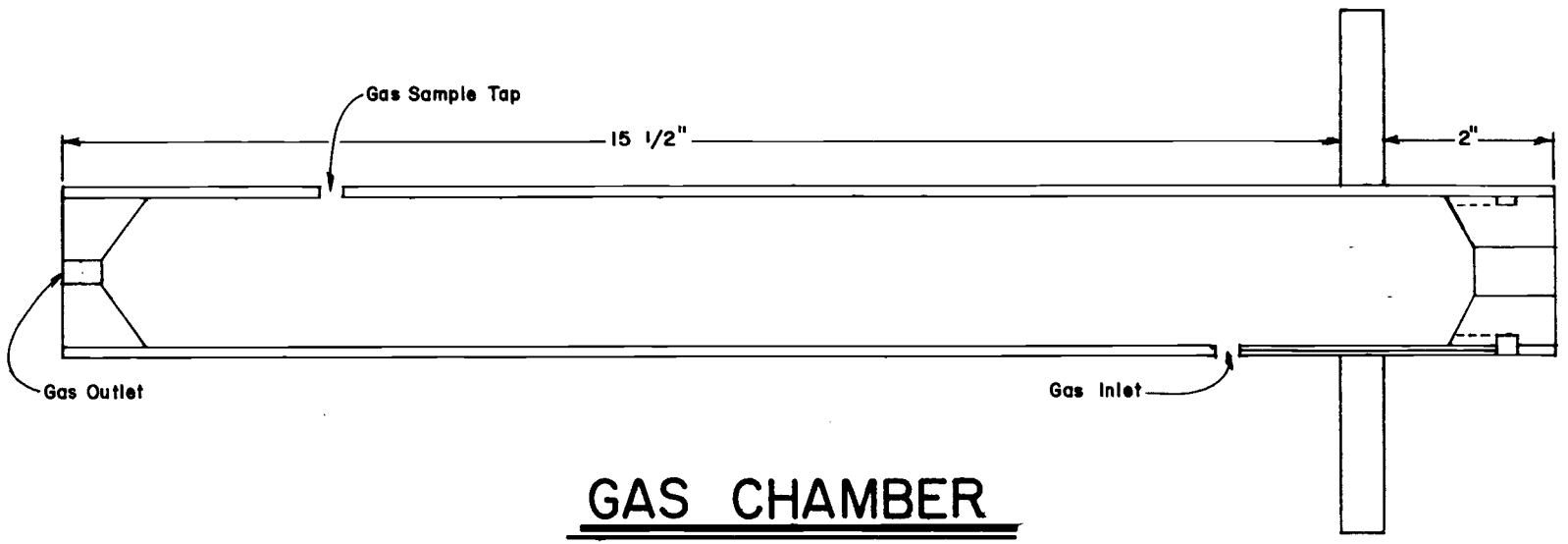

GAS CHAMBER

Scale: 1" = 2"

Figure 6. Gas chamber.

inches long.

The gas feed tank, which is item E in Figure 3, was the same type vessel as the absorbing liquid storage reservoir. The top of this carboy was also closed with a two-hole rubber stopper, through which passed the polyethylene gas feed line and a glass nipple three inches long.

The effluent liquid receiver, which is item B in Figure 3, was also a 13 gallon, Nalgene, Polyethylene carboy, but with a 1/2-inch bottom outlet spigot. The top of this carboy was closed with a number 13 1/2, three-hole rubber stopper through which passed three short glass nipples.

The gas displacement liquid storage vessel, which is item D in Figure 3, was the same type of a carboy as the effluent liquid receiver. The stopper on this carboy was the same as the stopper on the absorbing liquid storage reservoir.

The liquid overflow reservoir, which is item F in Figure 3, was a three gallon, narrow mouth, glass carboy, which was open to the atmosphere. The gas displacement liquid overflow reservoir, which is item N in Figure 3, was a two gallon, narrow mouth, glass carboy open to the atmosphere. This latter carboy was kept in the hood. Also used in the experimental work was a 20 liter, narrow mouth, glass carboy for mixing the salt solutions.

Flow Control

The liquid constant head overflow assembly, which is item G in Figure 3, was a glass tube with a bottom outlet and six overflow levels. The body of the constant head overflow assembly had a 9/32-inch inside diameter and an overall length of 45 inches. The overflow arms had an inside diameter of 5/32-inch and a length of three inches. The six overflow arms were three inches apart, center to center distance, and started at the top of the assembly. The top of the body was sealed so that the top overflow arm acted as a vent or siphon breaker. The bottom overflow arm was used for the absorbing liquid inlet. A thermometer with an outside diameter of 1/4-inch and an overall length of 18 inches was suspended in the body of this constant head overflow assembly.

The gas constant head overflow assembly, which is item O in Figure 3, was the same as the liquid constant head overflow assembly except for two modifications. The body was only 18 inches long and there was no thermometer suspended in the body of this unit.

The restrictions in the lines to control the flow rates of the liquid and gas were short glass tubes with a small internal diameter. These are items H and P in Figure 3 for the liquid and gas, respectively. Both liquid and gas units are the same with a large diameter restriction tube and a small diameter restriction tube. The

large diameter restriction tubes were six inches long with an inside diameter of 0.075 of an inch. The small diameter restriction tubes were six inches long with an inside diameter of 0.046 of an inch.

The gas displacement liquid standpipe, which is item S in Figure 3, was a glass pipe with an inside diameter of 1 1/2-inches and a height of 60 inches. The bottom was closed with a number eight, one-hole rubber stopper through which passed a glass nipple. The top of the standpipe was closed with a two-hole, number eight rubber stopper, through which passed two short glass nipples.

Sample Valves

The sample valves on the gas inlet and gas outlet lines, which are items L and M in Figure 3, respectively, were Varian, number 57-000169-00. Six-port sample valves with a one milliliter stainless steel sample loop. Figure 7 shows a sketch of the flow through the valves for the various valve positions. The sample valves were kept warm, by a 150 watt light bulb placed close to the sample loops, to prevent condensation in the sample loop. A curtain of polyethylene was hung in front of the sample valves to prevent them from being suddenly cooled by an air draft.

Constant pressure bypasses, which are items K and Q in Figure 3 were installed in parallel with the sample valves to avoid excessive pressure drop across the sample valves. The constant

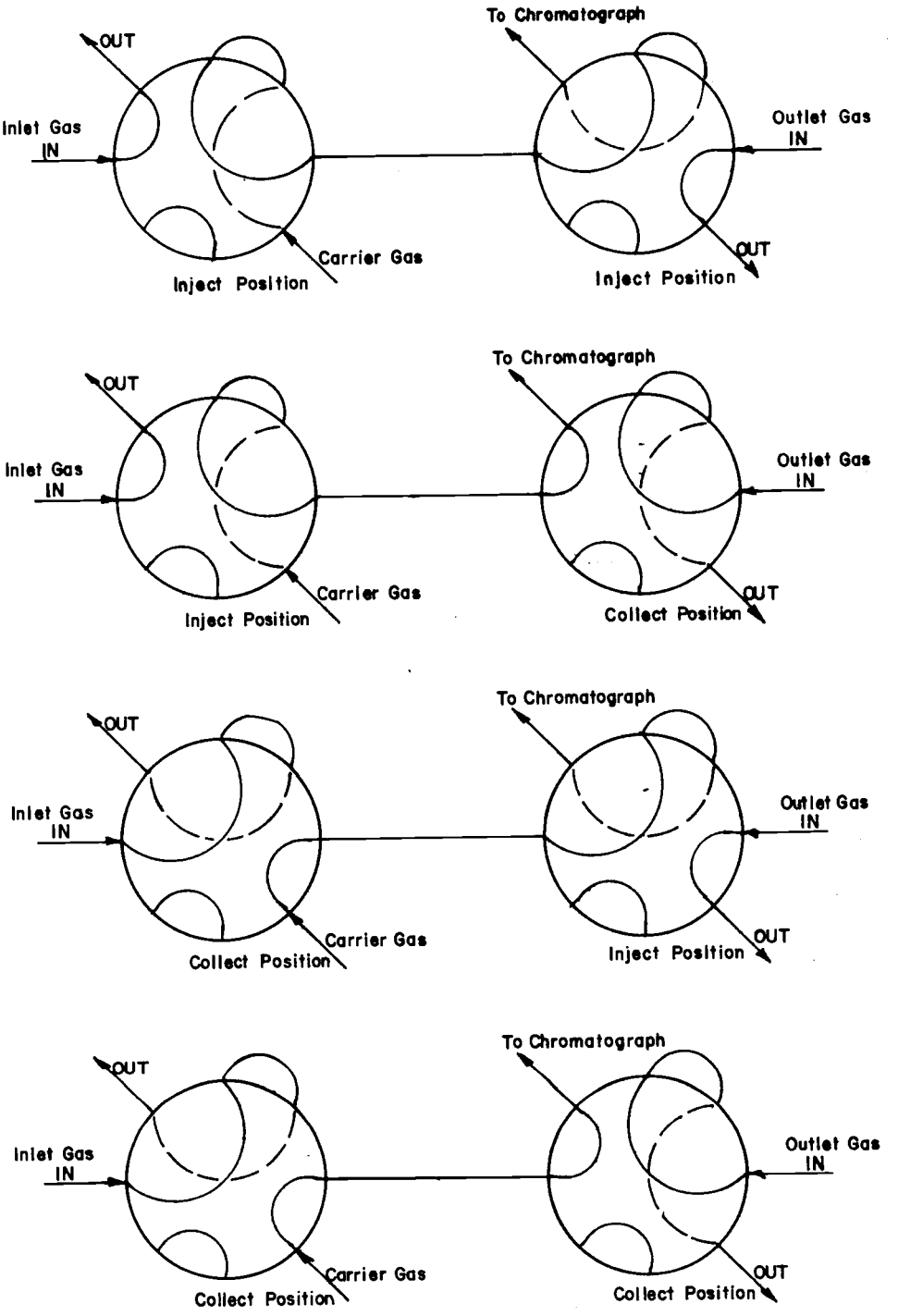

SAMPLE VALVE FLOW PATTERNS

Figure 7. Sample valve flow patterns.

pressure bypasses were 500 milliliter Erlenmeyer flasks with a fixed water level in the bottom. The tops of the flasks were closed with two-hole, number seven rubber stoppers, through which the inlet and outlet polyethylene tubing lines extended. The inlet lines extended to the bottom of the flasks where they were submerged in the water, but the outlet lines were extended only to the bottom of the rubber stopper.

Flows

The lines used in the system were as follows:

1. latex tubing with an inside diameter of 1/4-inch and outside diameter of 3/8-inch,
2. tygon tubing with an inside diameter of 1/4-inch and outside diameter of 3/8-inch,
3. plexiglass tubing with an inside diameter of 1/8-inch and an outside diameter of 1/4-inch,
4. polyethylene tubing with an outside diameter of 1/4-inch and an inside diameter of 1/8-inch,
5. teflon tubing with an outside diameter of 1/8-inch and a wall thickness of 0.030 of an inch.

The lines were blocked off with a Hoffman, opensided, one inch, screw compressor clamp.

The absorbing liquid flowed through latex tubing from the bottom of the absorbing liquid storage reservoir to the liquid constant head

overflow assembly. Flow was regulated with a Hoffman clamp to limit flow out the overflow arm to a relatively small amount. From the bottom of the constant head overflow assembly the absorbing liquid flowed through latex tubing to the restriction tubes. From the restriction tubes the absorbing liquid flowed through tygon tubing to the absorption tower. The liquid flowed up the inside of the stainless steel pipe and overflowed down the outside of it to form the wetted wall. The absorbing liquid flowed from the base of the absorption tower to the top of the effluent liquid receiver through tygon tubing. A latex gas equalizing line ran from the top of the effluent liquid receiver to the top of the gas space of the base assembly of the tower. A latex vent line was teed-off the latter line and ran to a back pressure controller in the hood which is item I in Figure 3. The backpressure controller was a 500 milliliter Erlenmeyer flask with an open top and a fixed water level. The vent line was submerged in the flask. The liquid collected in the effluent receiver was periodically drained between runs.

The overflow from the constant head overflow assembly ran through latex tubing to the top of the liquid overflow reservoir. A polyethylene line ran from the bottom of the liquid overflow reservoir out the top and into the suction of the liquid reservoir refill pump, which is item J in Figure 3. From the refill pump the liquid flowed through a latex line into the top of the absorbing liquid storage

reservoir.

The liquid reservoir refill pump was an Eastern Industries, Model E1, Assembly 60142, Type 100, 303 stainless steel pump, serial number C2F 0420, with a General Electric, model 5P56HC68, 115 volts, 60 cycle, 5000 RPM, 1/15 HP motor. A brass restrictor, with an opening 0.096 of an inch in diameter, was used to reduce the outlet pressure.

The gas displacement liquid flowed from the bottom of the gas displacement liquid storage vessel to the gas constant head overflow assembly through a latex line. The flow was regulated with a Hoffman clamp to provide a small amount of overflow from the constant head overflow assembly. The gas displacement liquid flowed from the bottom of the constant head overflow assembly to the restriction tubes through a latex line. From the restriction tubes, gas flowed into the top of the gas displacement liquid standpipe. The gas displacement liquid standpipe was vented to the atmosphere in the hood. From the bottom of the gas displacement liquid standpipe, the liquid flowed into the bottom of the gas feed tank.

The gas displacement liquid, flowing into the gas feed tank at a constant rate, forced gas from the gas feed tank at a constant flow rate. Gas flowed through polyethylene lines from the gas feed tank to the gas inlet sample valve and the constant pressure bypass. The gas then flowed through polyethylene lines to the gas inlet line of the

absorption tower. The exiting gas flowed out of the top of the absorption tower through polyethylene lines to the gas outlet sample valve and the constant pressure bypass and then on to the hood where it was vented to the atmosphere.

The gas displacement liquid overflow was pumped from the gas displacement overflow reservoir through tygon tubing that entered through the top of the carboy. The outlet from the pump flowed through a latex line to the top of the gas displacement liquid reservoir. The gas displacement liquid was pumped from the bottom of the gas feed tank through a latex line with the same pump.

The gas displacement liquid refill pump was an Eastern Industries, Model E1, assembly 60142, type 100, stainless steel pump with the serial number C1K 0155, which was driven by a General Electric, model 5P56HC68, 115 volts, 60 cycle, 1/15 HP, 5000 RPM motor. A brass restriction with a hole 0.076 of an inch in diameter was used to reduce the pump outlet pressure. The latex vent line from the gas displacement storage vessel was manifolded in such a manner that it could be used as an equalizing line with the gas feed tank when the gas displacement liquid was being pumped.

Temperatures were measured with Taylor Permafused, number 5991397 thermometers with a range of minus 1°C to 51°C and an immersion depth of 76 millimeters. To measure the liquid temperature, the thermometer was suspended in the body of the constant head

overflow assembly. The gas temperature measurement was taken with the thermometer suspended in the gas displacement liquid standpipe.

A line entered the liquid feed line to the absorption tower, between the restriction tubes and the tower, to add tap water to the system when the tower was not in use. This was done to keep the column wetted at all times.

The carrier gas flowed to the sample valve through a copper tubing, 1/8-inch in outside diameter. The carrier gas flowed between the two sample valves and on to the chromatograph through 1/8-inch teflon tubing.

Chromatograph

Analysis of the sample was done with a Wilkens Aerograph Gas Chromatograph, with a hydrogen flame ionization detector, model A-600-B, serial number 505. A Leeds and Northrup Speedomax H recorder, catalog number 3-961-000-186-6-030-5-66, serial number 62-20999-1-1 was used. Two chart speeds were available on the recorder, giving 30 inches per hour or 360 inches per hour chart travel. Six millivolt spans, which were 0 to 2, 0 to 5, 0 to 10, 0 to 25, 0 to 50, and 0 to 100, were available on the recorder. The column used in the chromatograph was five feet long, 1/8-inch in outside diameter, stainless steel tubing with a wall thickness of 0.030 of an

inch. This column was packed with five percent silicone grease, SE-30, on 60 to 80 mesh chromosorb W. Hydrogen flow from the hydrogen cylinder was approximately 18 milliliters per minute and was maintained with a pressure regulator and a capillary restriction tube. Premium pure bottled nitrogen carrier gas was used and a pressure of 11 pounds per square inch gauge was maintained at the cylinder outlet. This gave a carrier gas flow rate of approximately 28 milliliters per minute. Air for the hydrogen flame was taken from the Chemical Engineering Building air supply. A small stainless steel needle valve was used to maintain a constant air flow rate of approximately 350 milliliters per minute. The air flow rate was measured with a Brooks rotameter with a number 2-15-3 tube and a 1/8-inch glass float which gave a maximum capacity of about 500 milliliters per minute. The chromatograph column and detector were at a temperature of 51°C. The rheostat on the column temperature control was set at 31 and the rheostat on the injector temperature control was set at 40.

Equipment Modification for the Sulfur Dioxide System

The following modifications were made for the sulfur dioxide absorption runs. The sulfur dioxide gas was used directly from the sulfur dioxide cylinder and entered the system at the gas inlet sample valve constant pressure bypass. For the sulfur dioxide runs this

bypass was used primarily to saturate the gas with water as both sample valves were in a blocked off position for the sulfur dioxide runs.

The gas flow from the sulfur dioxide cylinder was controlled with a Matheson Co., Inc. pressure reducing regulator valve followed by a Matheson Co., Inc. number 104 needle valve. The needle valve was used to regulate the flow which was measured using a Brooks rotameter with a tube size R-2-15-A and with a 1/8-inch glass ball float. With the above exception the rest of the gas flow system was the same as for the mercaptan and sulfide gases.

The liquid side of the system was the same for the sulfur dioxide system as for the mercaptan and sulfide systems with the exception of a liquid effluent sampler. The liquid effluent sampler was installed between the outlet of the column and the effluent liquid receiver. The liquid effluent sampler is shown in Figure 8. About 20 milliliters of liquid could be held in the effluent sampler between the overflow arm and the sample valve.

Chemicals

The distilled water used in the experiment was made in a Barnstead still in the Chemical Engineering Building.

The chemicals used in this work were as follows:

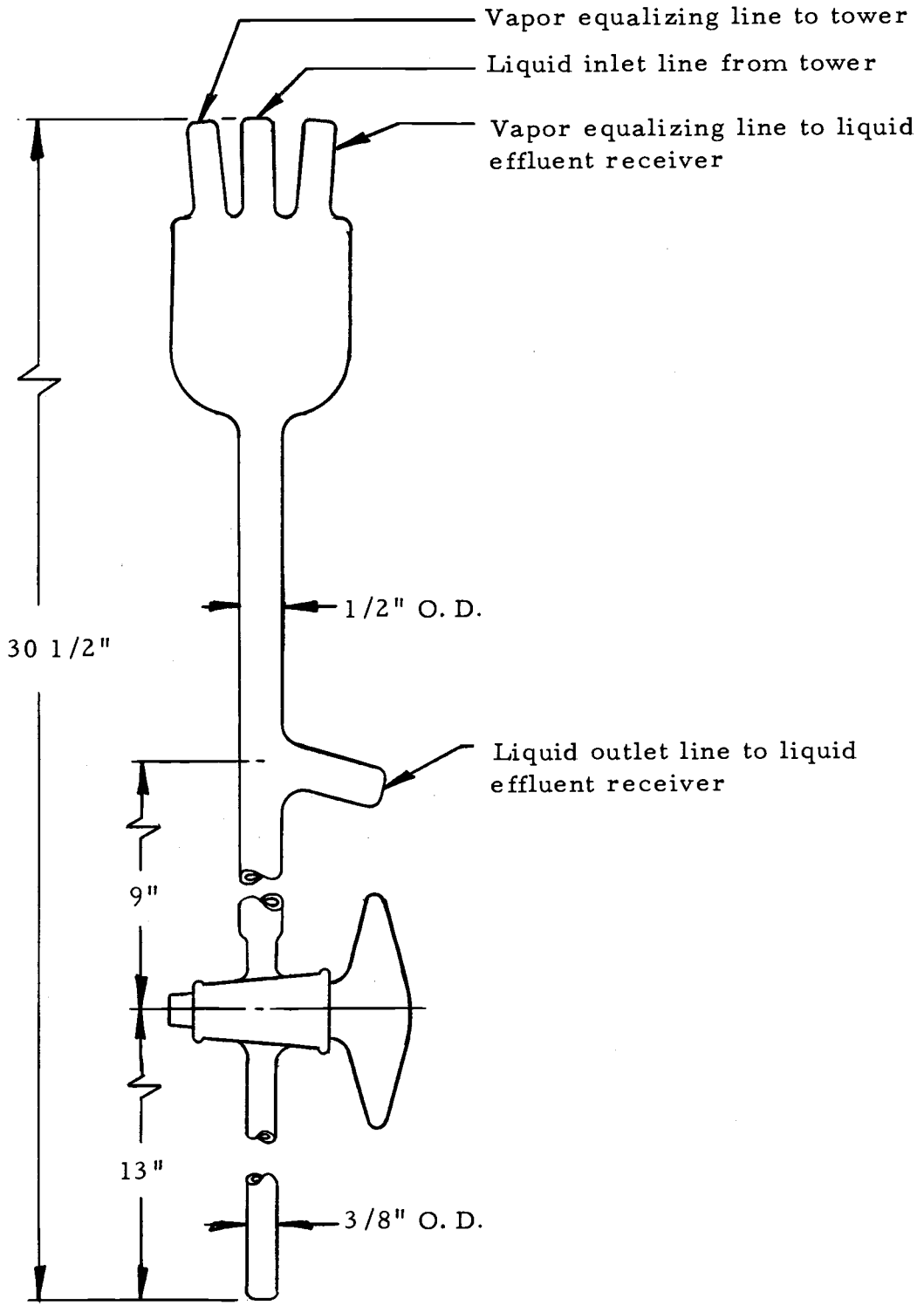

Figure 8. Liquid effluent sampler for the sulfur dioxide system.

Sodium hydroxide: Mallinckrodt's analytical reagent grade pellets.

Methyl mercaptan: Eastman's number 1795 methanethiol, reagent grade.

Dimethyl sulfide: J. T. Baker's Number R106 methyl sulfide, reagent grade.

Dimethyl Disulfide: J. T. Baker's Number Q460 methyl disulfide, reagent grade.

Mercuric chloride: Mallinckrodt's analytical reagent grade.

Cupric sulfate: Mallinckrodt's analytical reagent grade with five molecules water of hydration.

Zinc chloride: Mallinckrodt's analytical grade.

Cupric chloride: Mallinckrodt's analytical grade with two molecules water of hydration.

Cadmium chloride: Baker and Adamson's reagent grade with 2 1/2 molecules water of hydration.

Ferric chloride: Baker and Adamson's reagent grade with six molecules water of hydration.

Lead chloride: Baker and Adamson's reagent grade.

Sulfur dioxide: Matheson Co., Inc. commercial grade cylinder, 99.9 percent minimum sulfur dioxide.

IV. EXPERIMENTAL PROCEDURE

The flow of absorbing liquid from the absorbing liquid storage reservoir to the liquid constant head overflow assembly was regulated so that only a small amount of liquid was flowing through the overflow arm. The number two and five overflow arms, as numbered from the bottom, were used in this experimental work. These arms had static heads of about 12 and 21 inches over the column inlet level, respectively. Both large and small flow restriction tubes were used with each of the overflow levels, to give four flow rates of liquid in the experimental work. These flow rates were approximately 35 milliliters per minute, 70 milliliters per minute, 130 milliliters per minute and 200 milliliters per minute.

Initially the column was wetted before the start of each series of runs by running the inlet liquid at maximum flow rate for several minutes. As the experimental work progressed, it was noted that the column was not always satisfactorily wetted, especially for the first run of the series when using the low liquid flow rates; accordingly, a modification of the experimental procedure was made to keep tapwater flowing over the column even when no runs were being made. With this modification the wetting appeared more uniform from run to run and no dry streaks were observed even with the low liquid flow rates.

The gas displacement liquid was prepared so that a sufficient

quantity of the specific sulfur compound being absorbed was dissolved in the distilled water to give a saturated solution at the partial pressure of the gas feed mixture. In this manner it was possible to maintain a constant feed gas composition, and avoid changes in gas feed rate which would be introduced by gas absorption or desorption in the gas feed tank.

The gas displacement liquid for the methyl mercaptan runs contained about 0.3 of a gram of methyl mercaptan per liter of distilled water. The gas displacement liquid for the dimethyl sulfide runs contained about 0.4 of a gram of dimethyl sulfide per liter of distilled water. The gas displacement liquid for the dimethyl disulfide runs contained about 0.7 of a gram of dimethyl disulfide per liter of distilled water.

The flow of gas displacement liquid to the gas constant head overflow assembly was regulated with a Hoffman clamp to maintain a small amount of overflow from the desired overflow arm in the same manner as the liquid side. Only the numbers three, four, or five overflow arms, as numbered from the bottom, were used in the experimental work. These arms had static heads of 5 1/2, 8 1/2, and 11 1/2-inches, respectively, above the gas displacement liquid inlet into the standpipe. All three overflow levels were used with the large diameter flow restriction tube but only the numbers three and five overflow levels were used with the small diameter flow restriction

tube. This arrangement provided five gas flow rates of approximately 25 milliliters per minute, 40 milliliters per minute, 110 milliliters per minute, 150 milliliters per minute and 190 milliliters per minute. The liquid flowed into the top of the gas displacement liquid standpipe which was maintained at atmospheric pressure and from the bottom of the standpipe into the bottom of the gas feed tank. In order to maintain a constant flow of gas to the column a constant pressure bypass was installed around the sample valves. The liquid head in these constant pressure bypasses kept gas flowing through the sample valves, but allowed the excess gas to bypass the sample valve and thus prevent a buildup of back pressure on the system. Since there was a different pressure drop through the sample valves for the collecting and bypassing or injecting positions at a constant gas flow rate, the use of the constant pressure bypasses eliminated any pressure variations when switching the sample valve positions. For all except the lowest gas flow rate the sample valve was left in the inject or collect position for the entire three minute period when switching valve positions. For the lowest gas flow rate the sample valve was left in the inject position only 15 seconds. This was necessary since all of the gas feed could go through the valve when it was in the inject position but not when it was in the collect position.

When liquid was pumped from the gas feed tank to the gas displacement liquid reservoir the vent line was manifolded so that it was

open only between these two tanks; as a result the gas which filled the gas feed tank would be in equilibrium with the gas displacement liquid. At the start of each series of runs about five to ten liters of the gas displacement solution was in the gas feed tank. A series of runs was then made with displacement fluid continually added to the feed gas tank until the tank contained about 40 to 50 liters of liquid, at which time the series of runs was terminated. At the end of a series of runs the vent line on the gas displacement liquid storage vessel was blocked off in such a manner that it now served as an equalizing line with the gas feed tank. The liquid in the gas feed tank was then pumped to the gas displacement liquid storage vessel with the displacement liquid refill pump until only five to ten liters of gas displacement liquid remained in the gas feed tank.

A small amount of organic liquid was added to the gas displacement liquid reservoir between each series of runs to replace any organic liquid lost in the gas going to the column and that lost from the constant head overflow assembly and the standpipe vent. In the case of dimethyl sulfide and dimethyl disulfide the pure organic liquid was added from a pipet into the overflow reservoir before the reservoir was pumped to the gas displacement liquid storage reservoir. In the case of the methyl mercaptan a solution of 25 grams of methyl mercaptan in two liters of water was prepared and about 250 milliliters of this solution was added to the gas feed tank after it had been

essentially emptied, that is to a level of about five to ten liters. For the methyl mercaptan runs the next series of runs was not started until ten hours after the methyl mercaptan concentrate had been added to the feed tank. This time was provided to allow the gas and the liquid to equilibrate within the feed tank. Since the dimethyl sulfide and dimethyl disulfide were added to the gas displacement storage vessel only an hour was allowed for the gas feed tank to reach equilibrium before the next series of runs could be started. No significant change in feed composition was found during the runs.

A purge period was allowed at the start of each run. The purge period was one hour for the two lowest gas flow rates, 1/2-hour for the next two higher gas flow rates and 20 minutes for the highest gas flow rate. All runs lasted for one hour in addition to the purge period. The inlet and outlet gas streams were sampled alternately, every three minutes. The ten inlet and ten outlet samples were averaged to give an average analysis for both streams during the run. The concentration of the inlet and outlet streams was determined by measuring the area under the chromatograph peak and multiplying it by a calibration factor for converting area to concentration. Areas under the chromatograph curve were determined by measuring the sample peak height and multiplying it by the average width of the peak at one half of the height. The average width of the peak at one half of the height was determined by averaging the width obtained at the fast

chart speed for every third sample of each stream.

Flow rates were determined by measuring the levels of the displacement liquid in the gas feed tank and the effluent receiver tank every ten minutes for the duration of the run. A linear regression was made of the displacement readings to find the average displacement. The flow rate was then determined by multiplying the average displacement by the unit volume of the vessel. The regression coefficient for the flow rate of all of the runs was over 0.99.

The order of the runs within each block of runs was randomized by using a random number table. When absorbing with only distilled water, two or more blocks of runs were used. For the runs involving reacting liquid absorbing fluids only one block of runs was made.

During the investigation, the effect of salt solution on the dimethyl sulfide absorption was studied. Twenty liters of each salt solution was prepared with the following composition:

1. 0.0336 molar ferric chloride
2. 0.0190 molar mercuric chloride
3. 0.0229 molar cadmium chloride
4. 0.0279 molar cupric chloride
5. 0.0352 molar zinc chloride
6. 0.0066 molar lead chloride

Two flow rates were used with each solution. For the first condition, the gas flow rate was 110 milliliters per minute and the liquid flow

rate was 130 milliliters per minute. For the second condition, the gas flow rate was 190 milliliters per minute and the liquid flow rate was 35 milliliters per minute.

Three reacting solutions were used to absorb methyl mercaptan in the runs for evaluating the gas-side mass transfer coefficient. These solutions were

1. 0.3 molar caustic solution (runs 85-102)
2. 0.05 molar cupric sulfate solution (runs 103-111)
3. 0.1 molar caustic solution (runs 112-131).

The gas-side mass transfer coefficient for dimethyl sulfide was evaluated using a reacting solution of 0.05 molar mercuric chloride.

The liquid-side flow for the sulfur dioxide system was operated in the same manner as for the mercaptan and sulfide systems. The gas-side flow rate was set at a rotameter reading which gave a small amount of sulfur dioxide effluent gas from the system. One hour was allowed to purge any air or inert gas from the system. After the purge period a run was performed over a one hour period. Level displacement of the liquid was measured every ten minutes. Also every ten minutes an effluent liquid sample was taken.

TAPPI method T604-m-45 (41) was used for the analysis of the effluent liquid samples for total sulfur dioxide. The sample tap was submerged in the water in the volumetric flask while the sample was being collected rather than using a pipet to collect the sample as

specified in the above method. Fifty milliliters of distilled water was added to the volumetric flask from a pipet before collecting the sample. After the sample was collected the volumetric flask was filled to the mark from a buret and the sample size obtained as the difference in volume added and volume of the flask to the mark.

V. DATA ANALYSIS

The data taken to calculate the overall gas transfer coefficient included:

1. level of liquid effluent receiver, level of the liquid in the gas feed tank and the time at which the levels were measured,
2. temperature of the liquid flowing to the absorption tower,
3. temperature of the gas displacement liquid flowing to the gas feed tank,
4. the area under the peaks for the gas inlet and gas outlet samples,
5. effluent liquid analyses for the sulfur dioxide runs.

A least squares straight line was fit through the time versus level data for each of the tanks to get an average rate of change of the tank level. This rate of change was multiplied by the volume per centimeter of the tank to get the average gas and liquid feed rates for the run. Conversion factors and sources of physical properties are listed in Appendix D.

The area under the chromatograph peaks was measured in units such that there were 3600 square units per square inch. The areas were converted to a common basis by multiplying the measured area by the attenuation and the millivolt range of the recorder to get the unit area at 10^9 (ten to the ninth power) impedance. The conversion

factors for area at 10^9 impedance to concentration are given in Appendix D.

The method of calculation, as developed in the Theoretical Background Section, was used to calculate the Reynolds numbers and the mass transfer coefficients. The computer programs used in these calculations are shown in Appendix D.

For a wetted wall column of the type used there is the possibility that the end effects for the entrance and exit areas might have an influencing effect. Kramers and coworkers (20, 26) have studied the effects of entrance and exit regions and concluded that these effects are negligible after a distance of 20 times the film thickness has been traveled. In the present work the film thickness is between 0.0005 and 0.0010 feet while the length is 1.18 feet so entrance and exit effects have been neglected. Based on the work of Scriven and Pigford (38) the assumption of surface equilibrium is considered valid.

Since both the gas and liquid-side mass transfer coefficients were significant for the absorption of the mercaptans and sulfides in water, it was necessary to measure one phase resistance separately so that the other phase resistance could be calculated. To find the gas-side mass transfer coefficient for methyl mercaptan, sodium hydroxide and cupric sulfate solutions were used to absorb the methyl mercaptan to eliminate the effect of liquid-side resistance. Figure 9 shows a plot of overall mass transfer resistance versus gas phase

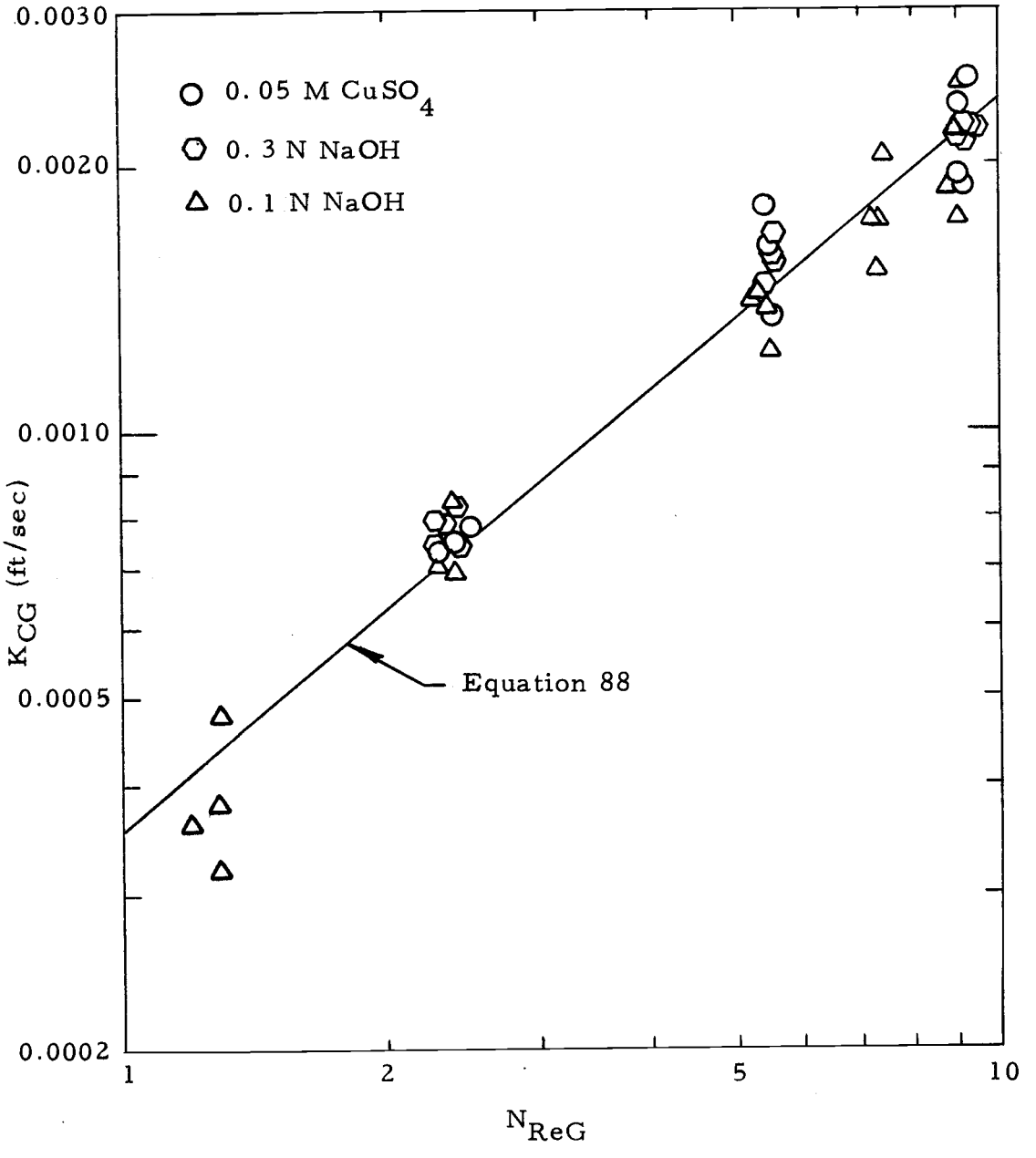

Figure 9. Overall mass transfer coefficient at various gas Reynolds numbers for methyl mercaptan being absorbed in reacting liquids.

Reynolds number. This plot shows that liquid phase Reynolds number does not effect the overall mass transfer coefficient; thus confirming the assumption, that for these solutions the liquid-side mass transfer resistance can be neglected. A least squares curve was fit to these data which gave the equation

$$\ln (k_{CG}) = -7.952 + 0.830 \ln (N_{ReG}) \tag{87}$$

or

$$k_{CG} = 3.5 \times 10^{-4} (N_{ReG})^{0.83} \tag{88}$$

with a correlation coefficient of 0.981 and a sample standard error (24) of 0.040 for $\ln (k_{CG})$ and a sample standard error of 0.024 for the exponent of the gas Reynolds number. The above least-squares-fit line is shown as the solid line on Figure 9.

Sharma and coworkers (31, 39) have studied the effect of gas Reynolds number or velocity on the gas phase mass transfer coefficient in a packed tower and in a bubble column and found the mass transfer coefficient proportional to gas Reynolds number to a power between 0.6 and 0.85. Reker and coworkers (36) have found that gas phase mass transfer coefficient was proportional to gas Reynolds number to the 0.83 power. It is felt that the relationship of Equation 87 is satisfactory in light of the other researchers work and the good fit of the data.

Several articles have been published which indicate mercuric chloride forms a complex with dimethyl sulfide (5, 7, 34). Based on these articles a series of runs was made to test the effect of mercuric chloride and several other chloride salts of heavy metals in an effort to find a suitable reacting liquid for absorbing dimethyl sulfide. As can be seen in Table 1 mercuric chloride was the only salt solution tested which gave a significant improvement in the overall mass transfer coefficient.

Table 1. Overall mass transfer coefficient for dimethyl sulfide into salt solutions.

Run	K_{CG}	N_{ReG}	N_{ReL}	Salt Solution
44	.000838	5.78	667	0.0336 M $FeCl_3$
45	.000778	9.31	191	0.0336 M $FeCl_3$
46	.001341	5.87	672	0.0190 M $HgCl_2$
47	.001186	9.27	203	0.0190 M $HgCl_2$
48	.000861	6.03	724	0.0229 M $CdCl_2$
49	.000751	9.29	232	0.0229 M $CdCl_2$
50	.000860	5.90	672	0.0279 M $CuCl_2$
51	.000708	9.33	222	0.0279 M $CuCl_2$
52	.000804	5.85	747	0.0352 M $ZnCl_2$
53	.000756	9.29	209	0.0352 M $ZnCl_2$
54	.000881	5.92	740	0.0066 M $PbCl_2$
55	.000799	9.30	211	0.0066 M $PbCl_2$
56	.000878	5.82	730	Distilled water
57	.000823	9.25	210	Distilled water

No information was found on an absorbing liquid which would react with dimethyl disulfide. Mercuric chloride was tried and found to be ineffective as a reacting liquid. Since the gas phase mass transfer coefficient for dimethyl disulfide could not be obtained directly, the gas phase mass transfer coefficients for the sulfides were obtained by ratioing the methyl mercaptan coefficients. Sharma and coworkers (31, 39) found that the mass transfer coefficients were proportional to the square root of diffusivity, and this relationship was used to obtain the gas phase mass transfer coefficients for the sulfide systems. This relationship is in agreement with the penetration model, as mentioned earlier in the Theoretical Background Section.

A series of runs using mercuric chloride as a reacting liquid to absorb dimethyl sulfide was performed to check the validity of ratioing the methyl mercaptan coefficients. Figure 10 shows the results of these runs and the solid line represents the coefficients obtained by ratioing the methyl mercaptan coefficients. It can be seen that the coefficient obtained by ratioing the methyl mercaptan coefficient represents a good fit of the experimental points. This was felt to be sufficient justification for using gas phase mass transfer coefficients obtained by ratioing for the two sulfide systems in the calculations of the liquid phase mass transfer coefficients.

Figure 11 shows the liquid mass transfer coefficient divided by the square root of diffusivity, $(k_L/\sqrt{D})$, which is the square root

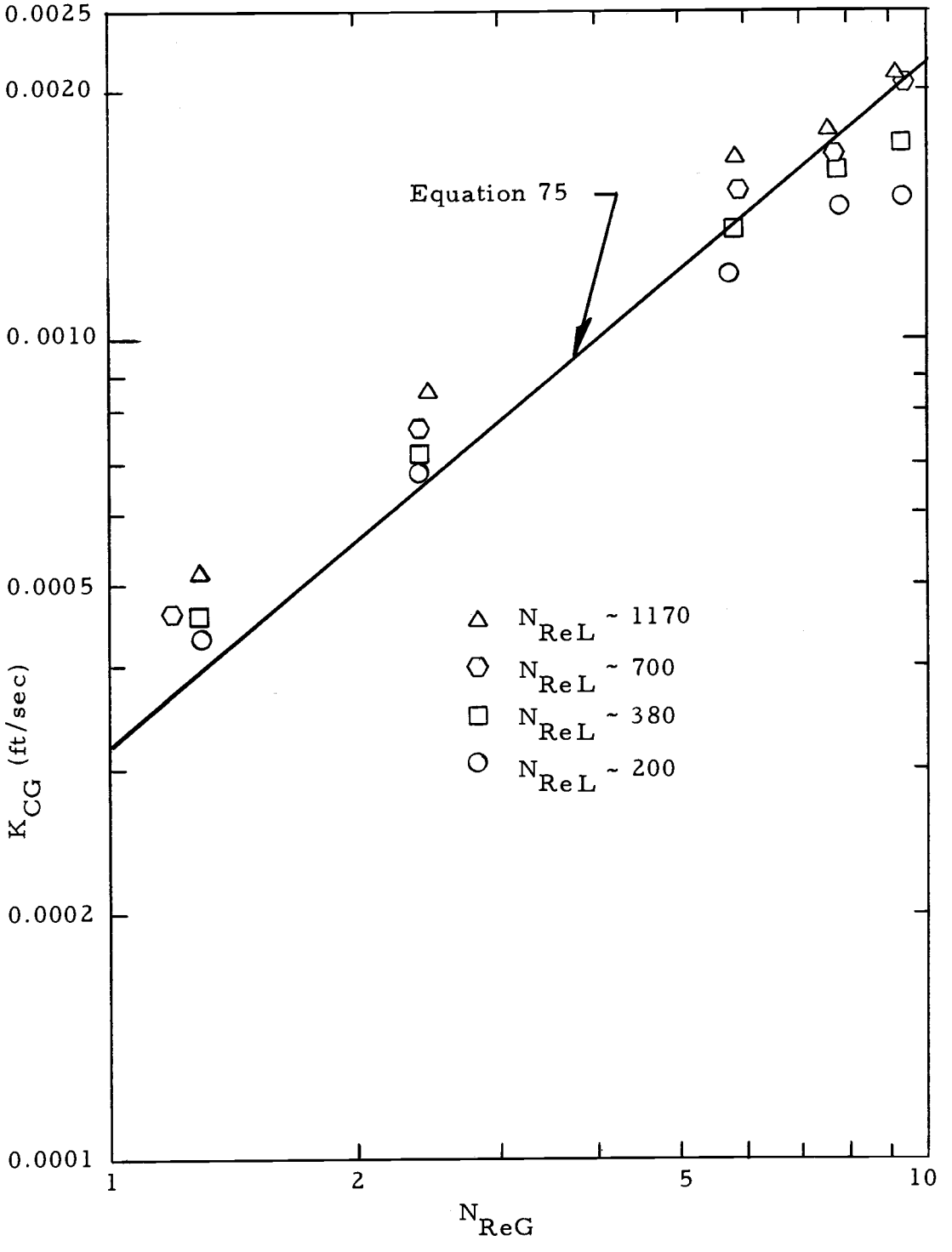

Figure 10. Overall mass transfer coefficient at various gas Reynolds numbers for dimethyl sulfide being absorbed in mercuric chloride.

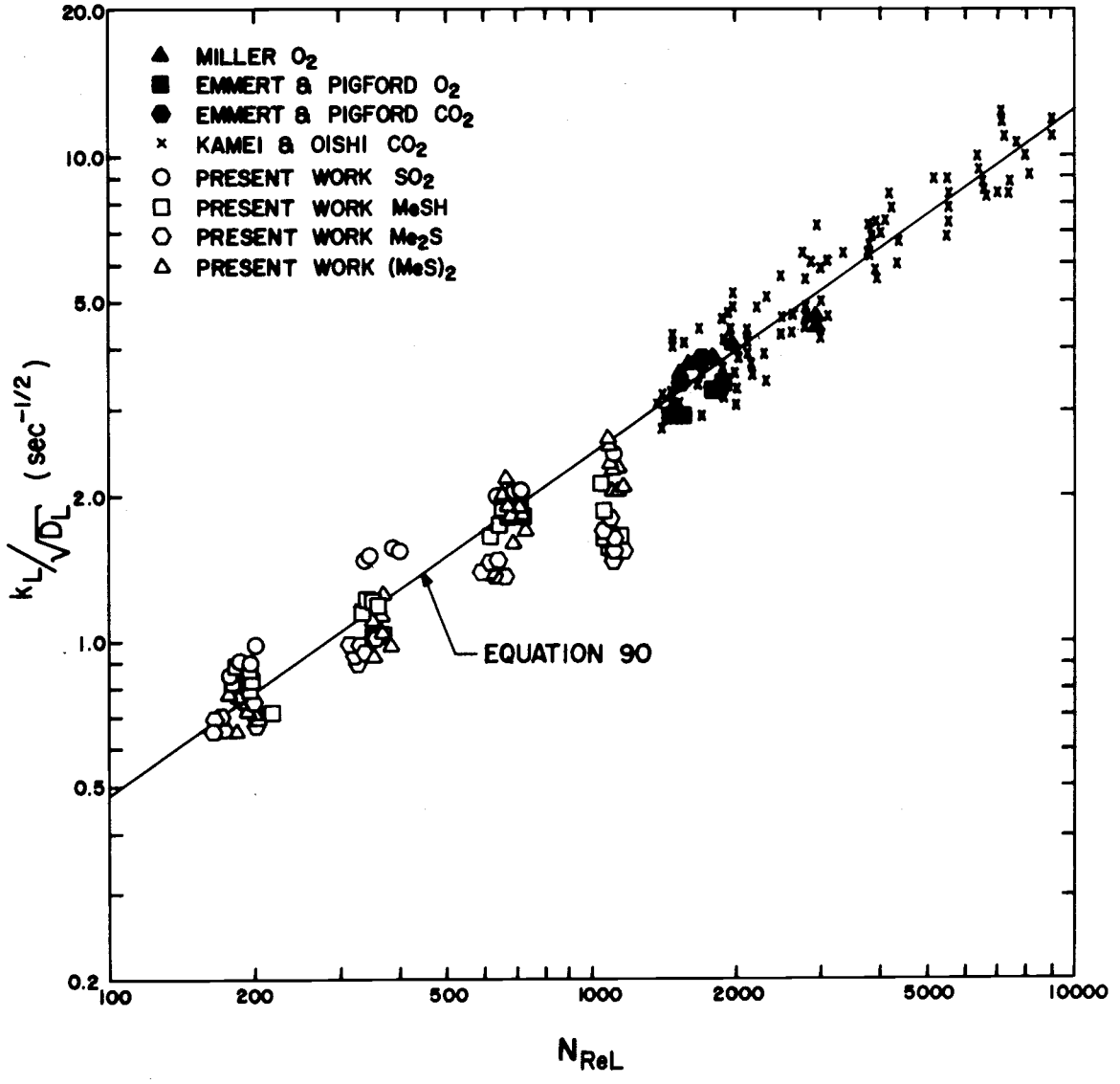

Figure 11. Liquid mass transfer coefficient divided by the square root of diffusivity at various liquid Reynolds numbers for all systems studied.

of surface renewal rate for the Danckwerts model, versus the liquid Reynolds number. This figure shows not only the present work but also the works of Emmert and Pigford, Kamei and Oishi, and Miller from the article by Banerjee (4). A least-square-fit straight line through all of the points had the following equation:

$$\ln\left(\frac{k_L}{\sqrt{D_L}}\right) = -3.934 + 0.695 \ln\left(N_{ReL}\right) \tag{89}$$

or

$$\frac{k_L}{\sqrt{D_L}} = 0.0196 \left(N_{ReL}\right)^{0.695} \tag{90}$$

The correlation coefficient was 0.943. The sample standard error was 0.121 and the sample standard error of the exponent of Reynolds number was 0.017. The least-squares-fit equation for the data from Banerjee's article only gave

$$\ln\left(\frac{k_L}{\sqrt{D_L}}\right) = -3.814 + 0.685 \ln\left(N_{ReL}\right) \tag{91}$$

which is within the sample standard error limits for both terms.

Figure 12 shows a plot of the liquid mass transfer coefficient divided by the square root of diffusivity, $(k_L/\sqrt{D})$, versus the liquid Reynolds number for the methyl mercaptan water system. The solid line represents the least-squares-fit line of the data in Figure 11. The data for the three highest gas flow rates agree quite well with the

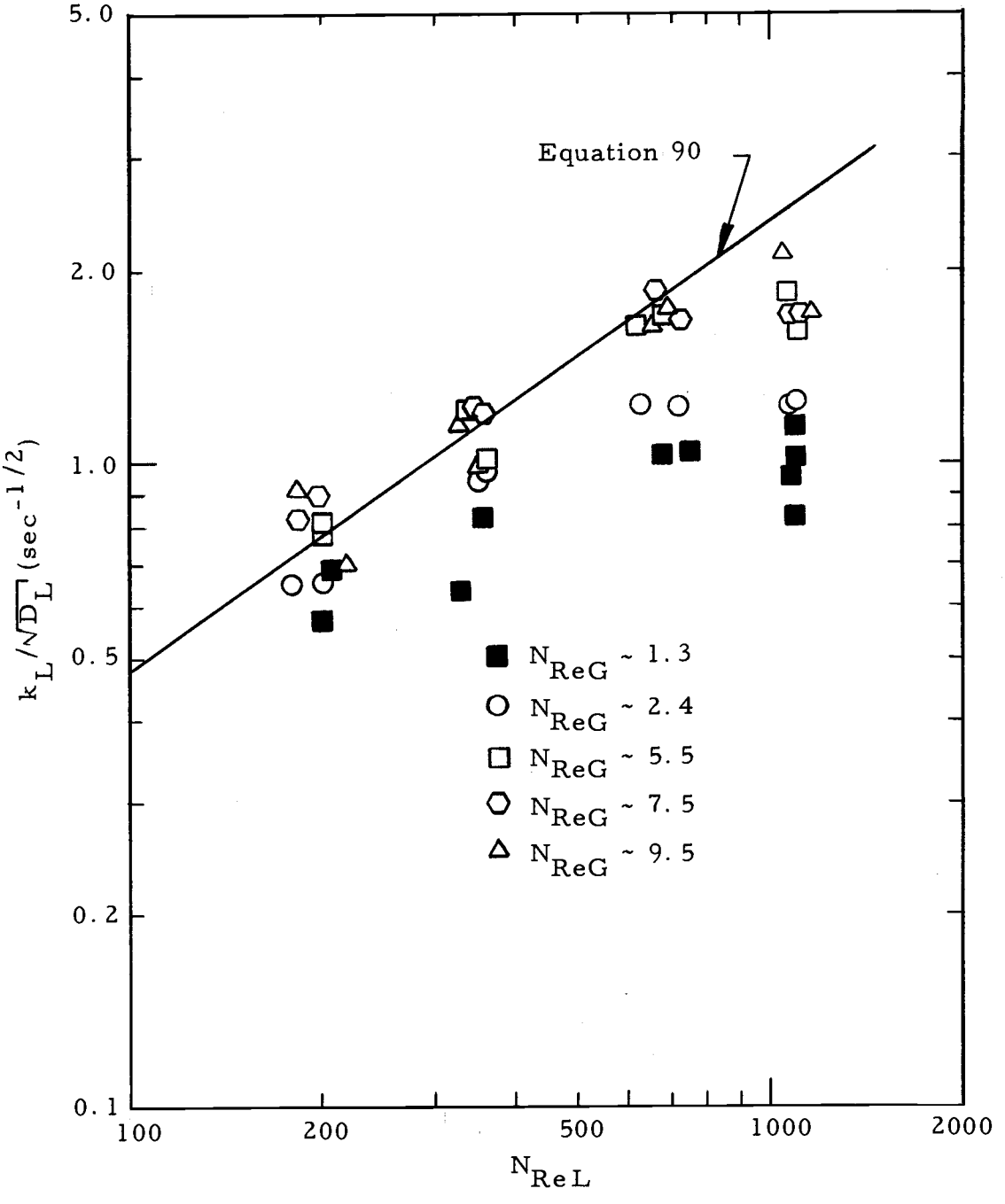

Figure 12. Liquid mass transfer coefficient divided by the square root of diffusivity at various liquid Reynolds numbers for methyl mercaptan-water system.

curve. It is felt that the gas transfer coefficient used for the two lowest gas flow rates was slightly high which would make the k_L points low. Examination of the data in Figure 9 indicates this is quite possible since most of the points at the low gas flow rates fall below the least-squares-fit straight line. The points representing the two lowest gas flow rates do not appear on Figure 11 because of the above probability of error. Figures 13 and 14 represent the plot of $(k_L/\sqrt{D'})$ versus liquid Reynolds number for dimethyl sulfide in water and dimethyl disulfide in water, respectively. These figures also indicate that the gas phase mass transfer coefficient for the two lowest gas flow rates were probably lower than the value used in the calculation. The values for the two lowest gas flow rates are not included in Figure 11, the same as for the methyl mercaptan system.

Figure 15 shows the plot of $(k_L/\sqrt{D'})$ versus liquid Reynolds number for the sulfur dioxide system. The liquid mass transfer coefficient for this system could be measured directly so less calculations and manipulation errors would be involved in this value. Also a different analysis method was used for this system so this gave an independent check of the analysis and calculation methods used for the other systems. The gas flow for runs number 313, 314, 319 and 322 were not great enough to provide all the sulfur dioxide the liquid could absorb in these runs and hence these four runs are not included in Figure 15.

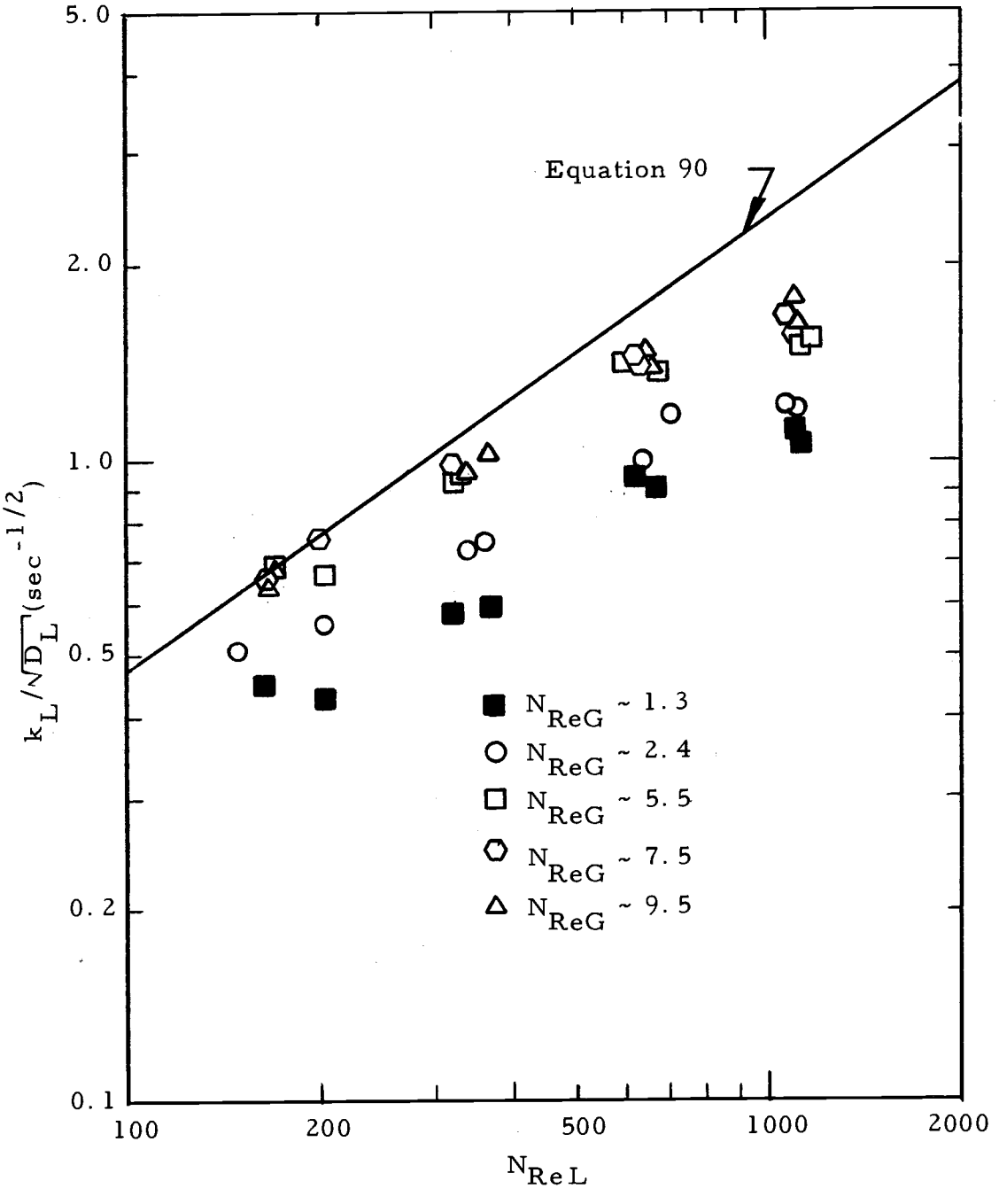

Figure 13. Liquid mass transfer coefficient divided by the square root of diffusivity at various liquid Reynolds numbers for dimethyl sulfide-water system.

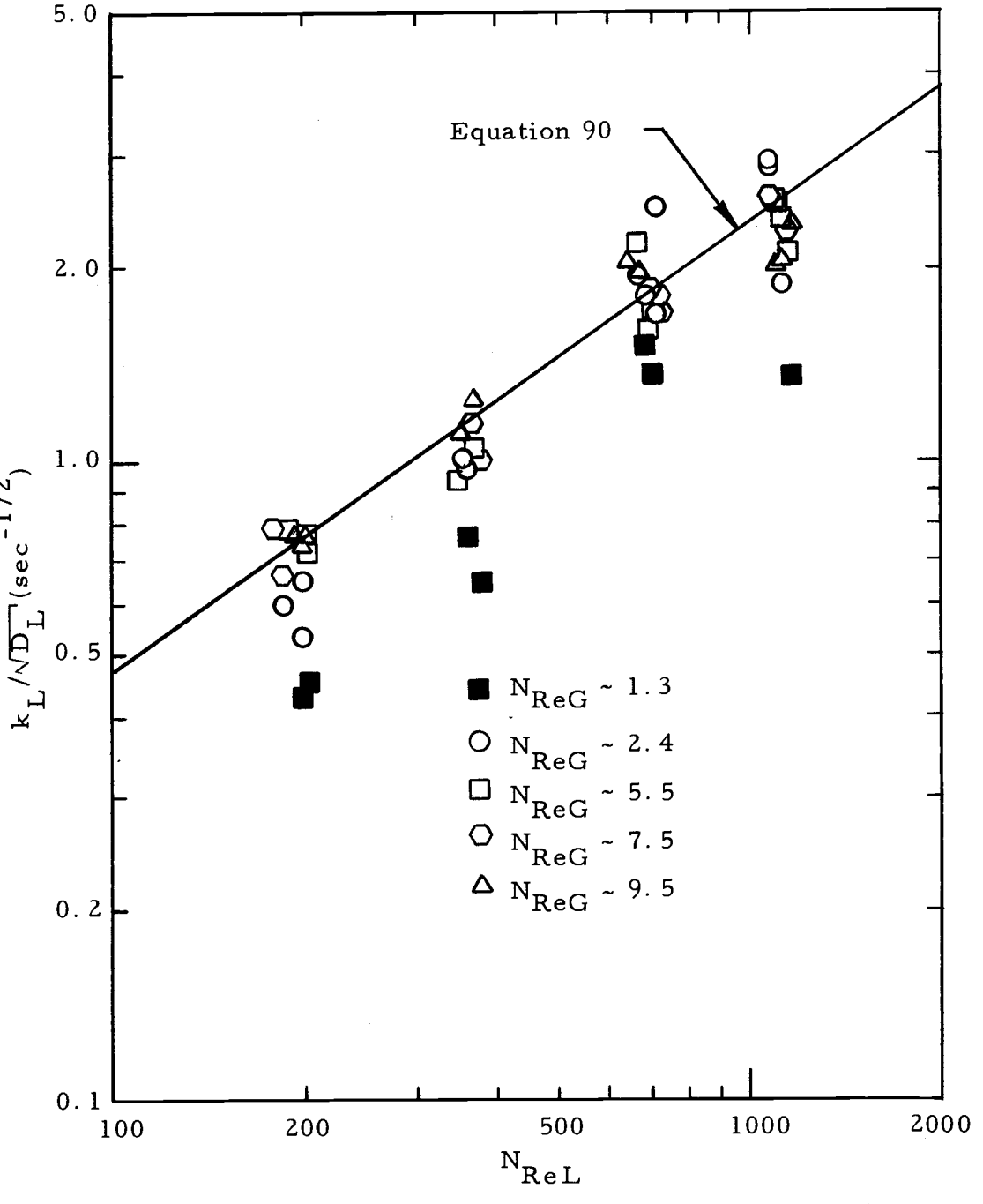

Figure 14. Liquid mass transfer coefficient divided by the square root of diffusivity at various liquid Reynolds numbers for dimethyl disulfide-water system.

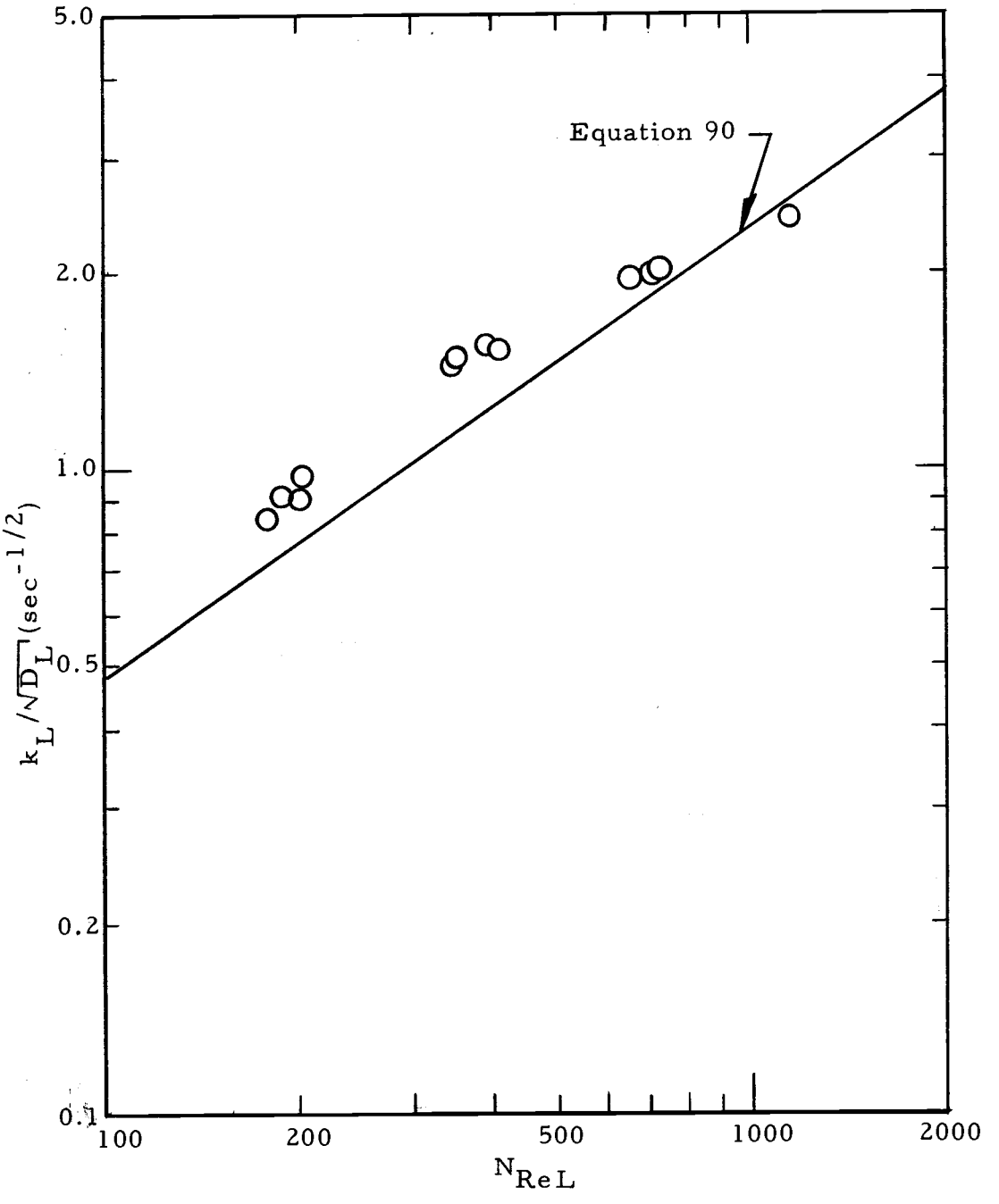

Figure 15. Liquid mass transfer coefficient divided by the square root of diffusivity at various liquid Reynolds numbers for sulfur dioxide-water system.

Banerjee and coworkers (4) have considered the surface renewal rate in light of eddies with a length l, and correlated this with the viscous energy dissipation. The viscous energy dissipation was then correlated with properties of the waves in a flowing film to get

$$k_L = f(\nu, N_{ReL}) \tag{92}$$

Banerjee evaluated Equation 92 using empirical equations for waves in water at room temperature to get

$$k_L = 2.93 \times 10^{-3} \sqrt{D} (N_{ReL})^{0.933} \tag{5}$$

However, using the data Banerjee presented, one finds the equation

$$k_L = 2.21 \times 10^{-2} \sqrt{D} (N_{ReL})^{0.685} \tag{93}$$

fits the data better. Equation 93 is the same as Equation 89 within the sample standard error for the combination of the work Banerjee presented and the present work. If one assumes the form of equation Banerjee developed

$$k_L = b_1 \nu^{1/6} D^{1/2} (N_{ReL})^{b_2} \tag{94}$$

is correct, then Equation 89 results on fitting b_1 and b_2 to the experimental data.

$$k_L = 0.133\ \nu_L^{1/6} D_L^{1/2} (N_{ReL})^{0.695} \qquad (95)$$

In development of the penetration model, Equations 43 and 44 show the square root of the surface renewal rate is equal to the phase mass transfer coefficient divided by the square root of the diffusivity in the phase.

$$\sqrt{s} = \frac{k}{\sqrt{D}} \qquad (96)$$

Combinations of Equations 95 and 96 and squaring both sides gives

$$s = (1.77 \times 10^{-2}) \nu^{1/3} N_{Re}^{1.390} \qquad (97)$$

Figure 16 is a plot of the gas phase mass transfer coefficient divided by the square root of diffusivity versus gas phase Reynolds number for the methyl mercaptan reacting liquid runs. The dashed line represents the extension of Equation 90 using the gas phase values rather than the liquid phase values. The solid line represents the square root of Equation 97.

The fit of Equation 97 is remarkable when one considers this is an extension of the Reynolds number range two orders of magnitude and a completely different system.

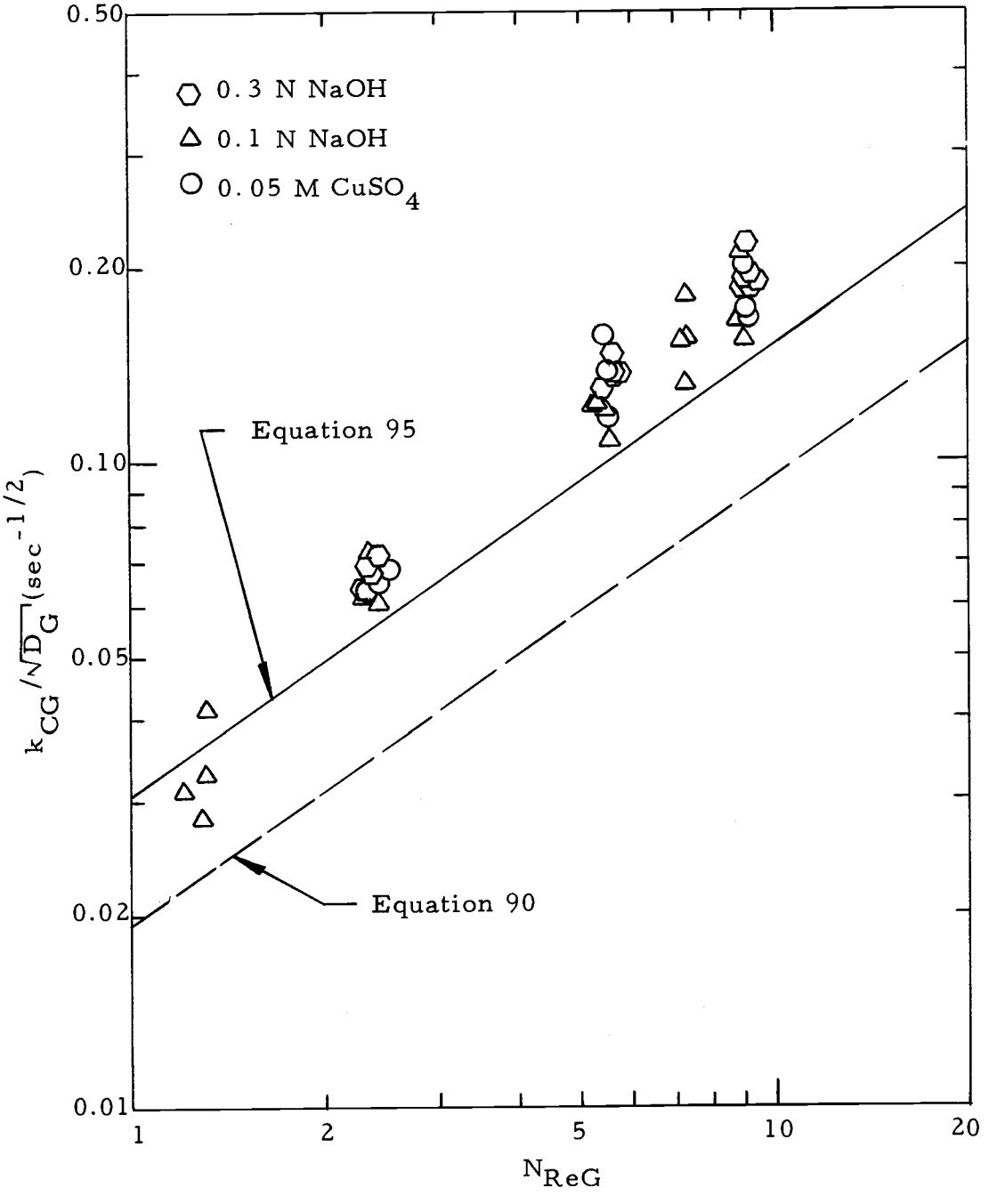

Figure 16. Gas mass transfer coefficient divided by the square root of diffusivity for methyl mercaptan-reacting liquid systems.

VI. SUMMARY

1. This study uses the form of the equation developed by Banerjee, but re-evaluates the constants in light of mass transfer results to obtain the empirical constants directly rather than from the empirical constants for wave motion.
2. This study extends the range over which liquid surface renewal rates are presented from the range of liquid Reynolds numbers of 1500 to 8500 presented in the paper by Banerjee. The present study adds the liquid Reynolds numbers of 200 to 1200 to give an expanded range of liquid Reynolds numbers from 200 to 8500.
3. The surface renewal equation is extended to include gas phase flow.
4. The use of gas phase flow extends the applicable range of the equation by two orders of magnitude to a lower limit of a gas Reynolds number of one.
5. This study extends the data to include the systems,
   a) dimethyl sulfide - air - water
   b) dimethyl sulfide - air - mercuric chloride
   c) dimethyl disulfide - air - water.
6. This study shows that the published equilibrium values for the dimethyl sulfide - water and dimethyl disulfide - water

systems are not reliable. Henry's law constants were measured by the National Council for Stream Improvement under the direction of the author, which verified this conclusion.

7. This study presents data for the mass transfer coefficients for dimethyl sulfide and dimethyl disulfide in air and water. These data had not previously been measured.
8. With the liquid systems investigated in this study the removal of the various sulfur compounds by absorption would be no better than the similar work reported by Oloman and coworkers.

VII. CONCLUSIONS AND RECOMMENDATIONS

Based on the work performed during the course of this project, the following conclusions and recommendations are offered.

Conclusions

1. The mass transfer coefficient for each phase can be expressed as $k = \sqrt{Ds}$ for the cases where the flow of one phase does not seriously effect the flow of the other phase.
2. The renewal rate, s, can be expressed as a function of Reynolds number and kinematic viscosity:

$$s = 0.0177\nu^{1/3}N_{Re}^{1.390}$$

for the cases where the flow of one phase does not seriously effect the flow of the other phase.

3. The surface renewal model is applicable for the range of Reynolds numbers from 1 to 8500.
4. The previously published data for the equilibrium of the systems dimethyl sulfide-water and dimethyl disulfide-water are not correct.

Recommendations for Further Work

1. The equilibrium for the systems dimethyl sulfide-water, dimethyl disulfide-water and methyl mercaptan-water needs to be studied further.
2. Diffusivity data on the systems dimethyl sulfide-water, dimethyl disulfide-water and methyl mercaptan-water need to be obtained.
3. The surface renewal rate needs to be determined for systems with higher gas flow rates to determine if the relationship presented in this work applies to those cases with an appreciable amount of momentum transfer across the gas-liquid boundary.
4. The surface renewal rate needs to be studied for cases of shorter columns to see when entrance effects become significant.

BIBLIOGRAPHY

1. Astarita, G., C. Balzano and F. Gioia. Hydrogen sulphide absorption in aqueous monoethanol amine solutions. Chemical Engineering Science 20:1101-1105. Dec. 1965.

2. Astarita, G. and F. Gioia. Hydrogen sulphide chemical absorption. Chemical Engineering Science 19:963-971. 1964.

3. Astarita, G. and F. Gioia. Simultaneous absorption of hydrogen sulfide and carbon dioxide in aqueous hydroxide solutions. Industrial and Engineering Chemistry - Fundamentals 4(3):317-320. Aug. 1965.

4. Banerjee, S., E. Rhodes and D. S. Scott. Mass transfer to falling wavy liquid films in turbulent flow. Industrial and Engineering Chemistry - Fundamentals 7(1):22-27. Feb. 1968.

5. Bassette, R. and C. H. Whitnah. Removal and identification of organic compounds by chemical reaction in chromatographic analysis. Analytical Chemistry 32:1098-1100. 1960.

6. Bird, R. B., W. E. Stewart and E. N. Lightfoot. Transport phenomena. New York, Wiley, 1965. p. 37-41, 511, 746.

7. Brown, H. C. and D. H. Wheeler. The effects of the steric requirements of the leaving group on the direction of bimolecular elimination in 2-pentyl derivatives. Journal of the American Chemical Society 78:2199-2202. 1956.

8. Carter, C. N. Effects of pH and oxidizing agents on the rate of absorption of hydrogen sulfide into aqueous media. TAPPI 50:329-334. July 1967.

9. Chen, Ning Hsing and D. F. Othmer. New generalized equation for gas diffusion coefficient. Journal of Chemical and Engineering Data 7:37-41. Jan. 1962.

10. Danckwerts, P. V. Significance of liquid-film coefficients in gas absorption. Industrial and Engineering Chemistry 43(6):1460-1467. June 1951.

11. Doraiswamy, L. K. and K. A. Reddy. Estimating liquid diffusivity. Industrial and Engineering Chemistry - Fundamentals 6(1):77-79. Feb. 1967.

12. Douglass, I. B. and L. Price. A study of methyl mercaptan and dimethyl sulfide formation in kraft pulping. TAPPI 49:335-342. Aug. 1966.

13. Gioia, F. and G. Astarita. General solution to the problem of hydrogen sulfide absorption in alkaline solutions. Industrial and Engineering Chemistry - Fundamentals 6(3):370-375. Aug. 1967.

14. Godfrey, J. H. Diffusion coefficients of binary gas systems: carbon tetrachloride - air, carbon tetrachloride - nitrogen, methyl sulfide - nitrogen, methyl disulfide - nitrogen. Master's thesis. Corvallis, Oregon State University, 1969. 41 numb. leaves.

15. Harkness, A. C. and B. A. Kelman. Solubility of methyl mercaptan in water. TAPPI 50:13. Jan. 1967.

16. Higbie, R. The rate of absorption of a pure gas into a still liquid during short periods of exposure. Transactions of the American Institute of Chemical Engineers 31:365-389. 1935.

17. Hrutfiord, B. F. and J. L. McCarthy. SEKOR I: Volatile organic compounds in kraft pulp mill effluent streams. TAPPI 50:82-85. Feb. 1967.

18. Jensen, G. A., D. F. Adams and H. Stern. Absorption of hydrogen sulfide and methyl mercaptan from dilute gas mixtures. Air Pollution Control Association Journal 16:248-253. May 1966.

19. Knudsen, J. G. and D. L. Katz. Fluid dynamics and heat transfer. New York, McGraw-Hill, 1958. p. 93, 186.

20. Kramers, H., R. H. Hendriksz and R. A. T. O. Nijsing. Absorption of CO_2 in jets and falling films of electrolyte solutions, with and without chemical reaction. Chemical Engineering Science 10:88-104. Apr. 1959.

21. Landry, J. E. The effect of a second order chemical reaction on the absorption of methyl mercaptan in a laminar liquid jet. Doctoral dissertation. Louisiana State University, 1966. 176 numb. leaves. Ann Arbor, Michigan, University Microfilms, Inc.

22. Lange, N. A. Handbook of chemistry. 8th ed. Sandusky, Ohio, Handbook Publishers, Inc., 1952. p. 1702-1708.

23. Leonardos, G., D. Kendall and N. Barnard. Odor threshold determination of 53 odorant chemicals. Journal of the Air Pollution Control Association 19:91-95. Feb. 1969.

24. Li, J. C. R. Introduction to statistical inference. Ann Arbor, Michigan, Edwards Brothers, Inc., 1957. p. 36.

25. Ljunggren, G. and B. Norberg. The effect and toxicity of dimethyl sulfide. Acta Physiologica Scandinavica 5:248-255. 1943 (Abstracted in Chemical Abstracts 38-5970[2]. 1944)

26. Lynn, S., J. R. Straatemeier and H. Kramers. Absorption studies in the light of the penetration theory. Chemical Engineering Science 4:58-62. Apr. 1955.

27. Maahs, H. G., L. N. Johanson and J. L. McCarthy. SEKOR III: Preliminary engineering design and cost estimates for steam stripping Kraft pulp mill effluents. TAPPI 50:270-275. June 1967.

28. Matteson, M. J., L. N. Johanson and J. L. McCarthy. SEKOR II: Steam stripping of volatile organic substances from kraft pulp mill effluent streams. TAPPI 50:86-91. Feb. 1967.

29. McKean, W. T., B. F. Hrutfiord and K. V. Sarkanen. Kinetic analysis of odor formation in the kraft pulping process. TAPPI 48:699-704. Dec. 1965.

30. McCabe, J. and W. W. Eckenfelder, Jr. Biological treatment of sewage and industrial wastes - Volume 1, aerobic oxidation. New York, Reinhold, 1956. p. 141-148.

31. Mehta, V. D. and M. M. Sharma. Effect of diffusivity on gas-side mass transfer coefficient. Chemical Engineering Science 21:361-365. Apr. 1966.

32. Oloman, C., F. E. Murray and J. B. Risk. The selective absorption of hydrogen sulfide from stack gas. Pulp and Paper Magazine of Canada 70:69-74. Dec. 5, 1969.

33. Perry, J. H. Chemical engineers handbook. 3rd ed. New York, McGraw-Hill, 1950. p. 204.

34. Phillips, F. C. Compounds of methyl sulphide with halides of metals. Journal of the American Chemical Society 23:250-258. Apr. 1901.

35. Reid, E. E. Organic chemistry of bivalent sulfur. Vol. 1. New York, Chemical Publishing, 1958. p. 131.

36. Reker, J. R., C. A. Plank and E. R. Gerhard. Liquid surface area effects in wetted-wall column. AIChE Journal 12:1008-1010. Sept. 1966.

37. Sarkanen, K. V. et al. Kraft odor. TAPPI 53:766-783. May 1970.

38. Scriven, L. E. and R. L. Pigford. On phase equilibrium at the gas-liquid interface during absorption. AIChE Journal 4(4):439-444. Dec. 1958.

39. Sharma, M. M. and A. D. Vidwans. Gas-side mass transfer coefficient in packed columns. Chemical Engineering Science 22:673-684. Apr. 1967.

40. Shih, T. T. C. et al. Methyl mercaptan vapor-liquid equilibrium in aqueous systems as a function of temperature and pH. TAPPI 50:634-638. Dec. 1967.

41. Technical Association of the Pulp and Paper Industry, New York. TAPPI standards and suggested materials. Method number T604-m-45.

42. Welty, J. R., C. E. Wicks and R. E. Wilson. Fundamentals of momentum,heat and mass transfer. New York, Wiley, 1969. p. 463.

43. White, P. T., D. G. Barnard-Smith and F. A. Fidler. Vapor pressure-temperature relationships of sulfur compounds related to petroleum. Industrial and Engineering Chemistry 44:1430-1438. June 1952.

44. Whitman, W. G. The two film theory of gas absorption. Chemical and Metallurgical Engineering 29:146-148. July 23, 1923.

APPENDICES

A. HENRY'S LAW CONSTANTS EVALUATION FOR DIMETHYL SULFIDE AND DIMETHYL DISULFIDE

Equilibrium data for the dimethyl sulfide and dimethyl disulfide system were obtained by the National Council for Stream Improvement in the following manner:

1. Five hundred milliliters of water were added to each of four, one liter volumetric flasks which were then stoppered with a number four, one-hole rubber stopper which was wrapped in a thin film of polyethylene. The hole in the stopper was plugged with a number 1F sleeve type, rubber serum bottle stopper.
2. A given amount of the dimethyl sulfide or dimethyl disulfide was injected into the stoppered flask with either a number 705 or 725 Hamilton microliter syringe with capacities of 50 and 250 microliters (μl) respectively. The samples were as follows:

   Sample A 200 μl dimethyl sulfide

   Sample B 100 μl dimethyl sulfide

   Sample C 100 μl dimethyl disulfide

   Sample D 50 μl dimethyl disulfide
3. The samples were allowed to set for two weeks to attain equilibrium.

4. A 1/2-milliliter gas sample was taken with a Hamilton number 1002 gas-tight microliter syringe with a capacity of 2 1/2-milliliters. The sample was analyzed on a Barton titrator which had a 1400°C quartz ignition tube and an air flow of 250 milliliters per minute.
5. A 10 microliter liquid sample was taken from the dimethyl sulfide tubes and injected into the Barton titrator ignition tube.

The Barton titrator analyses for sulfur dioxide so it was necessary to divide the quantity by two to get the moles of dimethyl disulfide. As the concentration of the prepared samples was known it was possible to get an area to concentration factor for the Barton titrator. This allowed the dimethyl disulfide equilibrium to be calculated from only the gas phase analysis.

Sample A:

$$Me_2S = \frac{400\ \mu l}{\ell_{H_2O}} \; 0.\frac{846\ gm}{10^3\ \mu l} \; \frac{g\ Mole}{62.1\ gm} = 5.45 \times 10^{-3}\ \frac{g\ Mole}{\ell}$$

Average area on Barton titrator for 10 µl liquid sample = 0.80 sq in equivalent to $8.0 \times 10^4\ \frac{sq\ in}{\ell}$; for 0.5 ml gas sample = 3.98 sq in equivalent to $7.96 \times 10^3\ \frac{sq\ in}{\ell}$

$$H = \frac{C_G}{C_L} = \frac{7.96 \times 10^{3}}{8.00 \times 10^{4}} = 0.0995 \quad \text{at } 27°C$$

$$\frac{\text{g Mole}}{\text{area}} = \frac{5.45 \times 10^{-3}}{8.0 \times 10^{4}} = 6.81 \times 10^{-8}$$

Sample B:

$$Me_2S = \frac{200\ \mu l}{\ell\ H_2O} \quad \frac{0.846\ \text{gm}}{10^{3}\ \mu l} \quad \frac{\text{g Mole}}{62.1} = 2.72 \times 10^{-3}\ \frac{\text{g Mole}}{\ell}$$

Average area on Barton titrator for 10 µl liquid sample = 0.39 sq in equivalent to $3.9 \times 10^{4}\ \frac{\text{sq in}}{\ell}$; for 0.5 ml gas sample = 2.08 sq in equivalent to $4.16 \times 10^{3}\ \frac{\text{sq in}}{\ell}$

$$H = \frac{4.16 \times 10^{3}}{3.90 \times 10^{4}} = 0.1065 \quad \text{at } 27°C$$

$$\frac{\text{g Mole}}{\text{area}} = \frac{2.72 \times 10^{-3}}{3.9 \times 10^{4}} = 6.97 \times 10^{-8}$$

Average H for two samples 0.103 at 27°C.

Average $\frac{\text{g Mole}}{\text{area}} = 6.89 \times 10^{-8}\ \frac{\text{g Mole}}{\text{sq in}}$

Sample C:

$$(MeS)_2 = \frac{200\ \mu l}{\ell\ H_2O} \quad \frac{1.057\ \text{gm}}{10^{3}\ \mu l} \quad \frac{\text{g Mole}}{94.2\ \text{gm}} = 2.24 \times 10^{-3}\ \frac{\text{g Mole}}{\ell}$$

Since dimethyl disulfide has two moles sulfur per mole dimethyl disulfide the area factor will be $3.45 \times 10^{-8} \frac{\text{g Mole}}{\text{sq in}}$. For 0.5 ml gas sample the area on Barton was 1.86 sq inches equivalent to $3.72 \times 10^{3} \frac{\text{sq in}}{\ell}$. This gives a gas composition of $12.82 \times 10^{-5} \frac{\text{g Mole}}{\ell}$ so

$$H = \frac{12.82 \times 10^{-5}}{2.24 \times 10^{-3}} = \underline{0.0573} \quad \text{at } 27°\text{C.}$$

B. RELATIONSHIP OF INDIVIDUAL AND OVERALL MASS TRANSFER COEFFICIENTS

Figure 17 shows the concentration of solute in the gas, concentration of solute in liquid and the equilibrium between the vapor and liquid for a gas that obeys Henry's law. Point 1 represents the gas with the bulk composition C_G and the liquid with the bulk composition C_L. Since the gas obeys Henry's law the following relationships hold

$$C_G^* = HC_L \tag{61}$$

$$C_{Gi} = HC_{Li} \tag{98}$$

$$C_G = HC_L^* \tag{99}$$

In the Theoretical Background Section the following equations were defined for mass flux

$$N_A = K_{CG}(C_G - C_G^*) \tag{8}$$

$$N_A = K_L(C_L^* - C_L) \tag{9}$$

$$N_A = k_{CG}(C_G - C_{Gi}) \tag{10}$$

$$N_A = k_L(C_{Li} - C_L) \tag{11}$$

From the geometry of Figure 17 it can be seen that

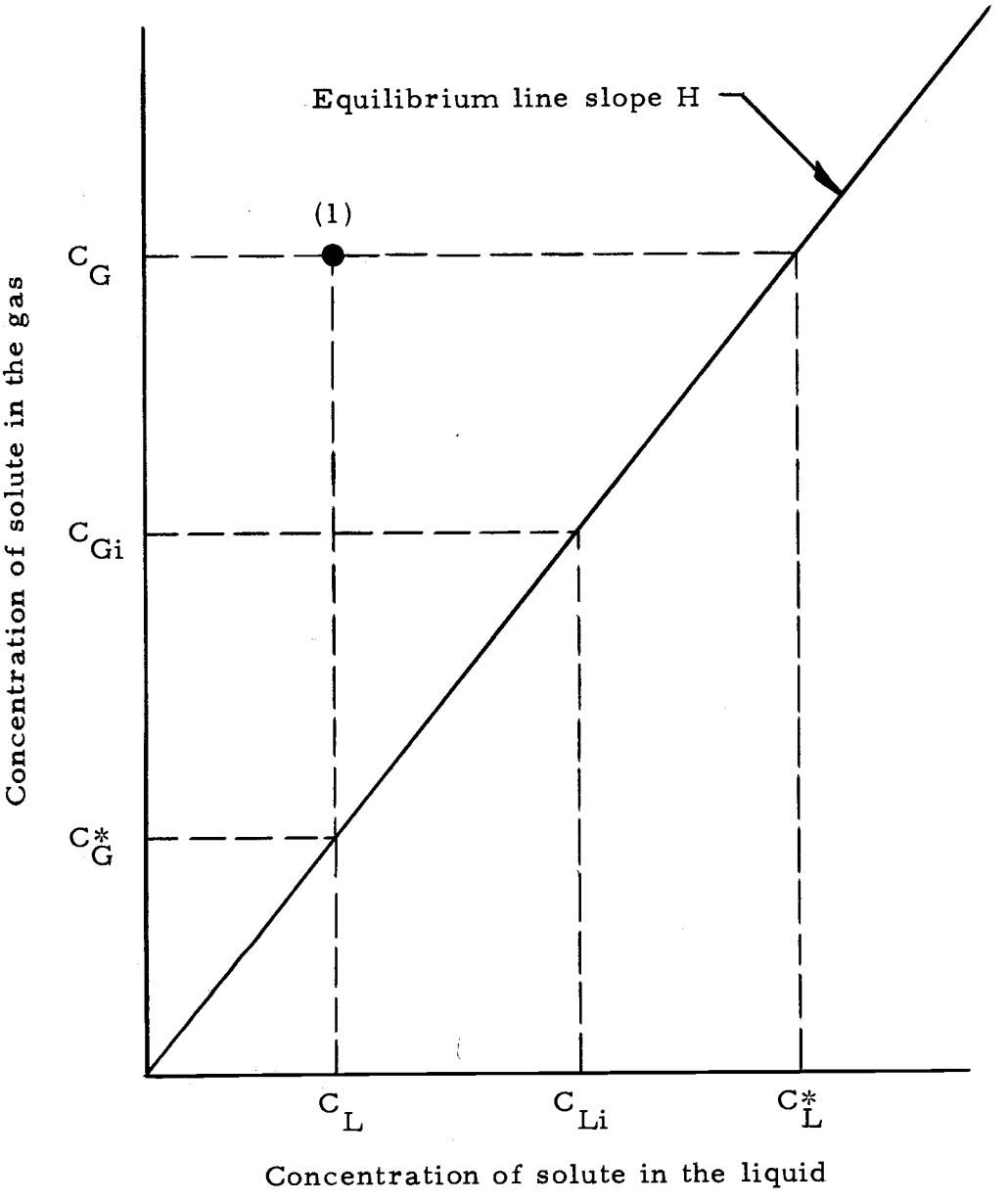

Figure 17. Equilibrium and operating line for liquid-gas contact.

$$(C_G - C_G^*) = (C_G - C_{Gi}) + (C_{Gi} - C_G^*) \tag{100}$$

Combining Equation 10 and Equation 11 the following is obtained

$$k_{CG}(C_G - C_{Gi}) = k_L(C_{Li} - C_L) \tag{101}$$

which gives

$$(C_G - C_{Gi}) = \frac{k_L}{k_{CG}} (C_{Li} - C_L) \tag{102}$$

The relationships of Equations 61 and 98 can be used to convert gas concentrations to liquid concentrations.

$$(C_{Gi} - C_G^*) = H(C_{Li} - C_L) \tag{103}$$

Substituting Equations 102 and 103 into Equation 100 gives

$$(C_G - C_G^*) = (C_{Li} - C_L)\left(\frac{k_L}{k_{CG}} + H\right) \tag{104}$$

Combining Equations 8, 11 and 104 gives

$$K_{CG}(C_{Li} - C_L)\left(\frac{k_L}{k_{CG}} + H\right) = k_L(C_{Li} - C_L) \tag{105}$$

This reduces to

$$\frac{1}{K_{CG}} = \frac{1}{k_{CG}} + \frac{H}{k_L} \tag{12}$$

By substituting Equations 61 and 99 into Equation 104 the following equation is obtained

$$H(C_L^* - C_L) = (C_{Li} - C_L)\left(\frac{k_L}{k_{CG}} + H\right) \tag{106}$$

Combining Equations 9, 11 and 106 gives

$$K_L \frac{(C_{Li} - C_L)}{H}\left(\frac{k_L}{k_{CG}} + H\right) = k_L(C_{Li} - C_L) \tag{107}$$

This reduces to

$$\frac{1}{K_L} = \frac{1}{Hk_{CG}} + \frac{1}{k_L} \tag{13}$$

C. DEVELOPMENT OF DANCKWERTS SURFACE RENEWAL FUNCTION

Danckwerts (10) postulated that the chance of an element of surface being removed from the surface would be independent of the elements age. The area of the surface is then

$$A = \int_0^\infty \varphi(t)dt \tag{108}$$

or if unit area is considered

$$1 = \int_0^\infty \varphi(t)dt \tag{109}$$

where $\varphi(t)dt$ is the fraction of the surface area with ages from t to $(t+dt)$. Consider two groups of ages $(t-dt)$ to t and t to $(t+dt)$. Let s be the rate of replacement of the surface which is returned to the turbulent core. For an increment of time so small that steady state can be assumed for the element, the following material balance can be made

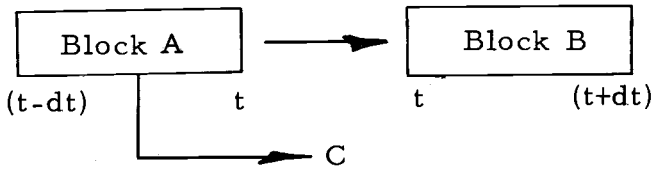

The amount going from block A to block B is the total contents of

block B which is, by the earlier definition, $\varphi(t)dt$. The amount returned to the turbulent core, C, is $(s\, dt\varphi(t-dt)dt)$; the renewal rate times the length of the time period times the original amount. The contents of block A is $\varphi(t-dt)dt$. For the geometry of the system

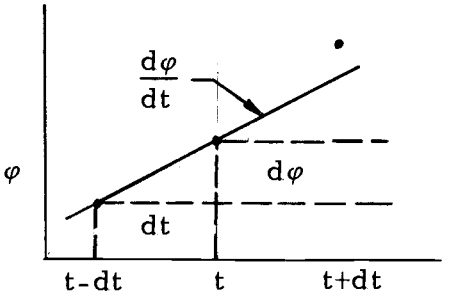

$$\varphi(t-dt) = \varphi(t) - \frac{d\varphi}{dt}dt \tag{110}$$

Expressing the material balance as a differential equation

$$\varphi(t-dt)dt = sdt\ \varphi(t-dt)dt + \varphi(t)dt \tag{111}$$

which upon making the substitutions for $\varphi(t-dt)$ gives

$$\varphi(t)dt - \frac{d\varphi}{dt}dt\ dt = sdt\ \varphi(t)dt - sdt\ \frac{d\varphi}{dt}dt\ dt + \varphi(t)dt \tag{112}$$

which reduces to

$$-d\varphi = s\varphi(t)dt - sdt\ d\varphi \tag{113}$$

and if $dt\ d\varphi$ is neglected as insignificant as compared to $d\varphi$ or dt

$$\frac{-d\varphi}{\varphi} = sdt \tag{114}$$

which solves to

$$\ln \varphi = -st + c_1 \tag{115}$$

or

$$\varphi = c_2 e^{-st} \tag{116}$$

c_2 can be evaluated from the knowledge that the sum of all fractions from $t = 0$ to ∞ is one or

$$1 = \int_0^\infty \varphi dt = \int_0^\infty c_2 e^{-st} dt \tag{117}$$

$$1 = c_2 \int_0^\infty e^{-st} dt = c_2 \, 1/s \tag{118}$$

so

$$c_2 = s \tag{119}$$

and

$$\varphi = se^{-st} \tag{38}$$

D. CALCULATIONS

Henry's law coefficients (H) were calculated as gas phase concentration divided by liquid phase concentration. The natural logarithm of H was expressed as a function of the reciprocal of temperature in degrees Kelvin to make adjustments for temperature change. Figure 1 shows the values of H for the methyl mercaptan system as the solid line. The values of H for dimethyl sulfide and dimethyl disulfide at 27°C used in this work were 0.103 and 0.0573, respectively. The change in H with temperature for the latter two compounds was taken to be the same as for the methyl mercaptan system.

Data for the viscosity and density of air and water solutions were taken from Lange's Handbook of Chemistry (22).

The gas diffusivities for dimethyl sulfide and dimethyl disulfide were based on the experimental measurements of Godfrey (14) and temperature adjustments were made using the equation developed by Chen and Othmer (9). The methyl mercaptan gas diffusivity was calculated using the Hirschfelder, Bird and Spotz (6) equation and the Chen and Othmer equation; the average value was used. These calculations are shown later in this section. The average of the values calculated by the Chen and Othmer and the Hirschfelder, Bird, and Spotz methods for dimethyl sulfide agreed very closely with the

experimental values of Godfrey.

The liquid diffusivities were calculated by the method proposed by Doraiswamy and Reddy (11) for the mercaptan and the sulfides. For the sulfur dioxide system the diffusivity of 1.83×10^{-8} square feet per second was taken from the work of Landry (21). Calculations of the liquid diffusivities are shown later in this section.

The required factor for converting the area under the chromatograph peak to concentration was determined by injecting 30 microliters of dimethyl sulfide into a one liter stoppered flask. The flask was allowed to set 48 hours before the gas was sampled with a microliter syringe and analyzed on the chromatograph. Samples were taken on several different days and an average area obtained. Since the volume of the flask and the amount of the dimethyl sulfide were known, the factor relating area to concentration was calculated. The factors for dimethyl disulfide and methyl mercaptan were obtained by ratioing the dimethyl sulfide factor using the ratios reported by Douglass (12). These ratios were for a hydrogen flame ionization detector which was operated at the same conditions as the one used in this experimental work. The factors used were as follows:

methyl mercaptan concentration equals area times 4.65×10^{-11}

dimethyl sulfide concentration equals area times 2.71×10^{-11}

dimethyl disulfide concentration equals area times 1.13×10^{-11}.

The gas feed tank and the liquid effluent tank had a displacement

of 959 and 950 milliliters per centimeter of height, respectively. The factors for converting displacement height per minute to cubic feet per second were 5.64×10^{-4} and 5.59×10^{-4}, respectively.

Gas diffusivities were calculated using the Hirschfelder, Bird and Spotz equation (6),

$$D_{12} = \frac{0.001858 T^{3/2} \left(\frac{1}{M_1} + \frac{1}{M_2}\right)^{1/2}}{P' \sigma_{12}^2 \Omega(1,2)^*} \tag{120}$$

$$^*\Omega(1,2) = f\left(\frac{kT}{\epsilon_{12}}\right) \tag{121}$$

and using the Chen and Othmer equation (9),

$$D_{12} = \frac{0.43 \left(\frac{T}{100}\right)^{1.81} \left[\frac{1}{M_1} + \frac{1}{M_2}\right]^{1/2}}{P' \left(\frac{T_{C1} T_{C2}}{10000}\right)^{0.1405} \left[\left(\frac{V_{C1}}{100}\right)^{0.4} + \left(\frac{V_{C2}}{100}\right)^{0.4}\right]^2} \tag{122}$$

$$\frac{\epsilon}{k} = 0.77 T_C \tag{123}$$

$$\sigma = 0.833 V_C^{1/3} \tag{124}$$

$$\left(\frac{\epsilon}{k}\right)_{12} = \left[\left(\frac{\epsilon}{k}\right)_1 \left(\frac{\epsilon}{k}\right)_2\right]^{1/2} \tag{125}$$

$$\sigma_{12} = \frac{\sigma_1 + \sigma_2}{2} \tag{126}$$

Property	Compound				
	Air	N_2	MeSH	Me_2S	$(MeS)_2$
M	29	28	48.1	62.1	94.2
T_C (33) °K	132.5	126.1	470	503	
ρ_C (33) $\frac{gm}{cc}$	0.35	0.311	0.323	0.306	
V_C $\frac{cc}{g\ Mole}$	82.8	90.1	148.9	203.	
σ	3.61	3.68	4.41	4.89	
ϵ/k	97.0	91.5	362	387	

Calculation of MeSMe-N_2 diffusivity at 296°K and 1 atmosphere

1. Using Hirschfelder, Bird and Spotz equation

$$\sigma_{12} = \frac{3.68 + 4.89}{2} = 4.28$$

$$\left(\frac{\epsilon}{k}\right)_{12} = [(91.5)(387)]^{1/2} = 188.2$$

$$\left(\frac{kT}{\epsilon}\right)_{12} = \frac{296}{188.2} = 1.571$$

$$\Omega_{12}\,(6) = 1.176$$

$$D_{12} = \frac{(1.858)(10^{-3})(296)^{3/2}\left[\frac{1}{28} + \frac{1}{62.1}\right]^{1/2}}{(1)(4.28)^2(1.176)}$$

$$D_{12} = 0.0996\ \frac{cm^2}{sec} = 1.071 \times 10^{-4}\ \frac{ft^2}{sec}$$

2. Using the Chen and Othmer equation for the same conditions

$$D_{12} = \frac{(0.43)(2.96)^{1.81}\left[\frac{1}{28} + \frac{1}{62.1}\right]^{1/2}}{(1)\left[(1.261)(5.03)\right]^{0.1405}\left[(0.901)^{0.4} + (2.03)^{0.4}\right]^2}$$

$$D_{12} = 0.1029 \frac{cm^2}{sec} = 1.107 \times 10^{-4} \frac{ft^2}{sec}$$

3. Experimental value from Godfrey (14)

$$D = 0.1016 \frac{cm^2}{sec} = 1.091 \times 10^{-4} \frac{ft^2}{sec}$$

Since the experimental value is between the values given by the two equations the average value of the two equations will be used for methyl mercaptan.

For the diffusivity of the Air-MeSMe, the diffusivity will be calculated by adjusting the N_2-MeSMe experimental value by both methods:

1. Using the Hirschfelder, Bird and Spotz method

$$\sigma_{12} = \frac{3.61 + 4.89}{2} = 4.25$$

$$\left(\frac{\epsilon}{k}\right) = \left[(97.0)(387)\right]^{1/2} = 193.7$$

$$\left(\frac{kT}{\epsilon}\right) = \frac{296}{193.7} = 1.530$$

$$\Omega_{12}\,(6) = 1.188$$

$$D_{12} = (0.1016)\left(\frac{4.28}{4.25}\right)^2\left(\frac{1.176}{1.188}\right)\frac{\left[\frac{1}{29}+\frac{1}{62.1}\right]^{1/2}}{\left[\frac{1}{28}+\frac{1}{62.1}\right]^{1/2}}$$

$$D_{12} = 0.1011\ \frac{cm^2}{sec} = 1.088 \times 10^{-4}\ \frac{ft^2}{sec}$$

2. Using the Chen and Othmer method

$$D_{12} = (0.1016)\frac{\left[\frac{1}{29}+\frac{1}{62.1}\right]^{1/2}}{\left[\frac{1}{28}+\frac{1}{62.1}\right]^{1/2}}\left(\frac{1.261}{1.325}\right)^{0.1405} \times \frac{\left[(0.901)^{0.4}+(2.03)^{0.4}\right]^2}{\left[(0.828)^{0.4}+(2.03)^{0.4}\right]^2}$$

$$D_{12} = 0.1040 = 1.119 \times 10^{-4}\ \frac{ft^2}{sec}$$

The average value of the two methods

$$D_{12} = \frac{(1.088+1.119)(10^{-4})}{2} = \underline{\qquad 1.104 \times 10^{-4}\ \frac{ft^2}{sec}}$$

for the dimethyl sulfide-air system at 296°K will be used.

Calculation of MeSH-Air diffusivity: at 296°K and 1 atmosphere

1. Using Hirschfelder, Bird and Spotz equation

$$\sigma_{12} = \frac{3.61+4.41}{2} = 4.01$$

$$\left(\frac{\epsilon}{k}\right)_{12} = [(97.0)(362)]^{1/2} = 187.4$$

$$\left(\frac{kT}{\epsilon}\right)_{12} = \frac{296}{187.4} = 1.578$$

$$\Omega_{12}(6) = 1.174$$

$$D_{12} = \frac{(1.858)(10^{-3})(296)^{3/2}\left[\frac{1}{29}+\frac{1}{48.1}\right]^{1/2}}{(1)(4.01)^{2}(1.174)}$$

$$D = 0.1176\ \frac{cm^2}{sec} = 1.262 \times 10^{-4}\ \frac{ft^2}{sec}$$

2. Using the Chen and Othmer equation for the same conditions,

$$D_{12} = \frac{(0.43)(2.96)^{1.81}\left[\frac{1}{29}+\frac{1}{48.1}\right]^{1/2}}{(1)\left[(1.325)(4.70)\right]^{0.1405}\left[(0.828)^{0.4}+(1.489)^{0.4}\right]^{2}}$$

$$D_{12} = 0.1261\ \frac{cm^2}{sec} = 1.358 \times 10^{-4}\ \frac{ft^2}{sec}$$

The average value for the two methods

$$D_{12} = \frac{(1.262+1.358)(10^{-4})}{2} = \underline{1.31 \times 10^{-4}\ \frac{ft^2}{sec}}$$

for methyl mercaptan-air system at 296°K will be used.

Calculation of MeSSMe-Air diffusivity: The experimental diffusivity found by Godfrey for MeSSMe-N_2 will be adjusted to the Air-MeSSMe system using the same average correction factor for σ_{12} and

Ω_{12} as for the MeSMe system, (1.023), and the molecular weight correction

$$D_{12} = (0.0817)(1.023)\left[\frac{\frac{1}{29}+\frac{1}{94.2}}{\frac{1}{28}+\frac{1}{94.2}}\right]^{1/2}$$

$$D_{12} = 0.0825\ \frac{cm^2}{sec} = 0.888 \times 10^{-4}\ \frac{ft^2}{sec}$$

The liquid diffusivities were calculated using the equation of Doraiswamy and Reddy (11) which is a refinement of the Wilke-Chang method.

$$D_{12} = \frac{10 \times 10^{-8} T\sqrt{M_B}}{\mu'(V_A V_B)^{1/3}} \quad \text{for} \quad \frac{V_B}{V_A} \leq 1.5 \tag{127}$$

$$D_{12} = \frac{8.5 \times 10^{-8} T\sqrt{M_B}}{\mu'(V_A V_B)^{1/3}} \quad \text{for} \quad \frac{V_B}{V_A} > 1.5 \tag{128}$$

Based on $T = 296°K$

$\mu' = 0.936$ ctps

$M_B = 18$; $\sqrt{M_B} = 4.24$

$V_B = 18.78$ cc/g Mole

$V_{A\ MeSH}(42) = 14.8+(4)(3.7) + 25.6 = 55.2$

$V_{A\ Me_2S} = (2)(14.8) + (6)(3.7) + 25.6 = 77.4$

$$V_{A\ (MeS)_2} = (2)(14.8) + (6)(3.7) + (2)(25.6) = 103.0$$

All three compounds have $\frac{V_B}{V_A} \leq 1.5$

$$D_{12} = \frac{(10\times10^{-8})(296)(4.24)}{(0.936)(V_A^{1/3})(18.78)^{1/3}} = \frac{5.03 \times 10^{-5}}{V_A^{1/3}}$$

MeSH $\quad V_A^{1/3} = 3.81$

$$D_{12} = \frac{5.03}{3.81} 10^{-5} = 1.32 \times 10^{-5} \frac{cm^2}{sec} = 1.42 \times 10^{-8} \frac{ft^2}{sec}$$

$Me_2S \quad V_A^{1/3} = 4.25$

$$D_{12} = \frac{5.03}{4.25} 10^{-5} = 1.18 \times 10^{-5} \frac{cm^2}{sec} = 1.272 \times 10^{-8} \frac{ft^2}{sec}$$

$(MeS)_2 \quad V_A^{1/3} = 4.69$

$$D_{12} = \frac{5.03}{4.69} (10^{-5}) = 1.07 \times 10^{-5} \frac{cm^2}{sec} = 1.153 \times 10^{-8} \frac{ft^2}{sec}$$

Computer Program for Calculating Transfer Coefficients and Reynolds Numbers for Mercaptan and Sulfide Systems

```
      PROGRAM DATANAL
      DIMENSION AA(6),BB(6),CC(6),FF(6),GMW(6)
      DIMENSION AG(6),AL(6)
      WRITE (21,105)
      WRITE (22,105)
      WRITE (23,105)
      WRITE (24,105)
      WRITE (25,105)
      WRITE (26,105)
  105 FORMAT (1H1,//////)
      DD=1.4487   $  EE=0.02236   $  GG=171.1   $  HH=0.486
      R=82.17     $  PI=3.14159   $  Z=1.18
      DC=0.5/12.
      AA(1)=7.5886   $  BB(1)=2795.   $  CC(1)=1.0767
      AA(2)=7.5886   $  BB(2)=2795.   $  CC(2)=1.0250
      AA(3)=7.5886   $  BB(3)=2795.   $  CC(3)=1.0000
      AA(4)=7.0374   $  BB(4)=2795.   $  CC(4)=1.0000
      AA(5)=7.0374   $  BB(5)=2795.   $  CC(5)=1.0000
      AA(6)=6.4510   $  BB(6)=2795.   $  CC(6)=1.0000
      FF(1)=1.011    $  GMW(1)=48.1
      FF(2)=1.004    $  GMW(2)=48.1
      FF(3)=1.000    $  GMW(3)=48.1
      FF(4)=1.000    $  GMW(4)=62.1
      FF(5)=1.000    $  GMW(5)=62.1
      FF(6)=1.000    $  GMW(6)=94.2
      AG(1)=0.0001310   $  AL(1)=0.0000000142
      AG(2)=0.0001310   $  AL(2)=0.0000000142
      AG(3)=0.0001310   $  AL(3)=0.0000000142
      AG(4)=0.0001104   $  AL(4)=0.0000000127
      AG(5)=0.0001104   $  AL(5)=0.0000000127
      AG(6)=0.0000888   $  AL(6)=0.0000000115
    9 READ (25,101) NRUN,QL,QG,CIN,COUT,TL,TG
  101 FORMAT (I3,2F7.7,2F8.8,2F3.1)
      IF (EOD(20)) GO TO 1
      I=7
      IF (NRUN.LE.102.AND.NRUN.GE.85) I=1
      IF (NRUN.LE.131.AND.NRUN.GE.103) I=2
      IF (NRUN.LE.173.AND.NRUN.GE.132) I=3
      IF (NRUN.LE.84.AND.NRUN.GE.58) I=3
      IF (NRUN.LE.292.AND.NRUN.GE.227) I=5
      IF (NRUN.LE.57.AND.NRUN.GE.13) I=5
      IF (NRUN.LE.47.AND.NRUN.GE.46) I=4
      IF (NRUN.LE.272.AND.NRUN.GE.253) I=4
      IF (NRUN.LE.226.AND.NRUN.GE.174) I=6
      IF (I.EQ.7) GO TO 9
      RHOGM=1./(1.314*(273.2+TG))
      RHOLM=3.44
      H=EXPF(AA(I)-BB(I)/(273.2+TL))
      VISL=CC(I)*(DD-EE*TL)*0.000674/(62.3*FF(I))
      DEL=(3.*QL*VISL/(PI*G*(DC+2.*((3.*QL*VISL/(PI*G*DC))**0.3333
     1))))**0.3333
      RENL=4.*QL/(VISL*(DC+2.*DEL))
      CINF=RHOGM
      YIN=CIN/RHOGM
      YOUT=COUT/RHOGM
      HNC=H
```

```
      IF (I.EQ.1) HNC=1
      IF (I.EQ.2) HNC=0
      IF (I.EQ.4) HNC=0
      CINL=0
      COUTL=QG*(CIN-COUT)/QL
      XIN=CINL/RHOLM
      XOUT=COUTL/RHOLM
      CNTOG=(1./(1.-HNC*QG/QL))*LOGF((CIN+HNC*QG/QL*(COUT-CIN))/
     1COUT)
      CKOG=CNTOG*QG/((DC+2.*DEL)*PI*Z)
      DIFG=(AG(I))*(((273.2+TG)/296.)**1.81)
      DIFGS=(AG(I))*(((273.2+TG)/296.)**1.81)
      DIFL=(AL(I))*(((273.2+TL)/296.)*0.936*0.000674)
     1/(VISL*62.4*FF(I))
      RHOGLB=2H03M*(GMW(I)*0.5*(YIN+YOUT)+(1.-0.5*(YIN+YOUT))*29.0)
      VISG=0.000002674*(GG+HH*TG)/RHOGLB
      R1=DC*0.5+DEL
      R2=1.5*0.5/12.
      RENG=2.*QG/(PI*(R2*R2-R1*R1))/(VISG*R2*LOGF(R2/R1))*(R1*R1+
     1R2*R2*(2.*LOGF(R2/R1)-1.))
      CKG=EXPF(0.830*(LOGF(RENG))-7.952)*((DIFG/DIFGS)**0.5)
      AKG=CKG/(DIFG**0.5)
      RENGR=RENG**0.8
      RENLR=RENL**0.8
      RENLVD=RENLR*((32.17*DEL)/(12.*VISL))
      CKL=H/(1./CKOG-1./CKG)
      AKL=CKL/(DIFL**0.5)
      WRITE (24,106) NRUN,CKG,AKG,RENGR
      WRITE (25,107) NRUN,CKL,AKL,RENLR,RENLVD
      WRITE (26,108) NRUN,CKOG,CKG,RENG,AKG,CKL,RENL,AKL
  108 FORMAT (5X,I3,4X,F10.6,4X,F10.6,4X,F6.2,4X,F7.3,4X,
     1F10.6,4X,F7.0,4X,F8.3)
      WRITE (27,108) NRUN,CKOG,CKG,RENG,AKG,CKL,RENL,AKL
  106 FORMAT (1H0,4X,I3,3F15.7)
  107 FORMAT (1H0,4X,I3,4F15.7)
      WRITE (21,102) NRUN,CIN,COUT,CINL,COUTL,TL,TG
      WRITE (22,103) NRUN,H,CKOG,RENL,RENG,CNTOG
      WRITE (23,104) NRUN,DEL,QL,QG,YIN,YOUT,XIN,XOUT
  103 FORMAT (1H0,4X,I3,F9.5,F11.7,2F14.5,F10.3)
  102 FORMAT (1HC,4X,I3,4F12.8,2F6.1)
  104 FORMAT (1H0,4X,I3,F9.5,2F10.7,4F8.5)
      GO TO 9
    1 CONTINUE
      END
```

Computer Program for Calculating Transfer Coefficient and Reynolds Numbers for Sulfur Dioxide System

```
      PROGRAM DATANALL
      DIMENSION AA(6),BB(6),CC(6),FF(6),GMW(6)
      DIMENSION AG(6),AL(6)
      WRITE (21,105)
      WRITE (22,105)
      WRITE (23,105)
      WRITE (24,105)
      WRITE (25,105)
  105 FORMAT (1H1,//////)
      DD=1.4467  $  EE=0.02226  $  GG=171.1  $  HH=0.486
      G=32.17    $  PI=3.14159  $  Z=1.18
      DC=0.5/12.
      AA(1)=5.04  $  BB(1)=2540.  $  CC(1)=1.  $  FF(1)=1.
      GMW(1)=64.  $  AL(1)=0.0000000183
    9 READ (20,101) NRUN,QL,QG,CIN,COUT,TL,TG
  101 FORMAT (I3,2F7.7,2F8.8,2F3.1)
      IF (EOD(20)) GO TO 1
      I=1
      RHOLM=3.44
      H=EXPF(AA(I)-BB(I)/(273.2+TL))
      VISL=CC(I)*(DD-EE*TL)*0.000674/(62.3*FF(I))
      DEL=(3.*QL*VISL/(PI*G*(DC+2.*((3.*QL*VISL/(PI*G*DC))**0.3333
     1))))**0.3333
      RENL=4.*QL/(VISL*(DC+2.*DEL))
      HNC=H
      XIN=CIN/RHOLM
      XOUT=COUT/RHOLM
      CSTAR=EXPF(-1.732-0.0313*TL)
      CNTOG=LOGF((CSTAR-CIN)/(CSTAR-COUT))
      CKOG=CNTOG*QL/((DC+2.*DEL)*PI*Z)
      DIFL=(AL(I))*(((273.2+TL)/296.)*0.936*0.000674)
     1/(VISL*62.4*FF(I))
      RENLA=RENL**0.8
      RENLVD=RENLA*((32.17*DEL)/(12.*VISL))
      CKL=CKOG
      AKL=CKL/(DIFL**0.5)
      WRITE (25,107) NRUN,CKL,AKL,RENLA,RENLVD
  107 FORMAT (1H0,4X,I3,4F15.7)
      WRITE (21,102) NRUN,CIN,COUT,TL,TG
      WRITE (22,103) NRUN,H,CKOG,RENL,CNTOG
      WRITE (23,104) NRUN,DEL,QL,XIN,XOUT
      WRITE (24,106) NRUN,CKOG,RENL,AKL
      WRITE (26,106) NRUN,CKOG,RENL,AKL
  106 FORMAT (5X,I3,4X,F10.6,4X,F7.0,4X,F8.3)
  103 FORMAT (1H0,4X,I3,F9.5,F11.7,F14.5,F10.3)
  102 FORMAT (1H0,4X,I3,2F12.8,2F6.1)
  104 FORMAT (1H0,4X,I3,F9.5,F10.7,2F8.5)
      GO TO 9
    1 CONTINUE
      END
```

E. DATA

Table 2. Data for the absorption of methyl mercaptan in 0.3 N sodium hydroxide.

	Temperature		Displacement Rate		Inlet Sample		Outlet Sample	
Run	Liquid °C	Gas °C	Liquid cm/min	Gas cm/min	Area*	Range mv	Area*	Range mv
85	23.3	23.0	0.1996	0.1207	8065	50	4387	2
86	23.8	23.4	0.1154	0.1989	7643	50	8447	2
87	24.6	23.4	0.0361	0.0493	7171	50	3192	2
88	23.7	23.1	0.1204	0.1211	8306	50	6244	2
89	24.1	23.4	0.0371	0.1211	7891	50	6245	2
90	24.7	23.8	0.1121	0.0511	7293	50	3375	2
91	25.1	24.1	0.0354	0.2021	7000	50	3531	5
92	24.9	22.8	0.2268	0.0500	6643	50	2237	2
93	24.8	23.5	0.2200	0.2000	6571	50	4770	2
94	24.1	23.3	0.0407	0.1975	6259	50	7672	2
95	24.1	23.6	0.2293	0.1989	8809	50	3877	5
96	24.7	23.5	0.1411	0.0486	8699	50	3513	2
97	25.3	24.1	0.2225	0.1189	8336	50	5568	2
98	25.7	24.5	0.0400	0.1200	7650	50	6119	2
99	23.3	22.2	0.1411	0.1164	7490	50	6331	2
100	23.9	22.5	0.0393	0.0521	6955	50	2546	2
101	24.9	23.3	0.2268	0.0507	6430	50	2374	2
102	25.4	23.8	0.1400	0.1950	5995	50	7183	2

*3600 square units per square inch.

Table 3. Data for the absorption of methyl mercaptan in 0.05 M cupric sulfate.

Run	Temperature		Displacement Rate		Inlet Sample		Outlet Sample	
	Liquid °C	Gas °C	Liquid cm/min	Gas cm/min	Area*	Range mv	Area*	Range mv
103	25.6	24.4	0.2289	0.0546	7302	50	3900	2
104	26.1	24.7	0.1446	0.0521	7017	50	3825	2
105	25.9	24.2	0.1454	0.1193	6940	50	8031	2
106	23.7	23.0	0.2275	0.1968	8015	50	4896	5
107	23.9	23.0	0.0371	0.0500	7533	50	3562	2
108	24.4	23.6	0.0379	0.1950	7081	50	4299	5
109	24.7	23.6	0.2286	0.1193	5840	50	2986	2
110	25.1	23.9	0.1439	0.1946	5641	50	2442	5
111	26.1	24.0	0.0400	0.1179	5574	50	5030	2

*3600 square units per square inch.

Table 4. Data for the absorption of methyl mercaptan in 0.1 N sodium hydroxide.

Run	Temperature		Displacement Rate		Inlet Sample		Outlet Sample	
	Liquid °C	Gas °C	Liquid cm/min	Gas cm/min	Area*	Range mv	Area*	Range mv
112	24.8	21.9	0.0411	0.0279	6551	50	1341	2
113	25.0	23.0	0.1454	0.0521	6290	50	1771	2
114	24.8	23.6	0.2293	0.1961	5981	50	4593	2
115	23.3	21.4	0.2268	0.0257	8242	50	4409	2
116	23.4	21.9	0.1407	0.1175	8039	50	8746	2
117	24.1	22.0	0.0371	0.0493	7380	50	3830	2
118	24.5	22.5	0.0714	0.0511	6849	50	4420	2
119	24.9	23.5	0.0436	0.1157	6476	50	6062	2
120	22.1	21.6	0.0696	0.1168	7066	50	4626	5
121	22.8	22.1	0.0400	0.1914	6700	50	7088	5
122	23.9	23.4	0.1489	0.0282	6210	50	7257	2
123	21.7	20.9	0.2318	0.1125	7688	50	6377	2
124	22.3	21.4	0.0693	0.1871	7220	50	5002	5
125	23.0	22.0	0.1449	0.1554	6661	50	8855	2
126	24.0	22.7	0.1493	0.1950	8369	50	4030	5
127	25.1	23.7	0.2311	0.0500	7985	50	3953	2
128	25.5	23.1	0.2329	0.1582	8334	50	6934	2
129	23.7	22.2	0.0400	0.1561	6707	50	9368	2
130	23.9	22.5	0.0757	0.1543	6318	50	8459	2
131	24.0	22.2	0.0707	0.0279	5914	50	3227	2

*3600 square units per square inch.

Table 5. Data for the absorption of methyl mercaptan in water.

Run	Temperature		Displacement Rate		Inlet Sample		Outlet Sample	
	Liquid °C	Gas °C	Liquid cm/min	Gas cm/min	Area*	Range mv	Area*	Range mv
132	20.8	21.8	0.2296	0.0261	5182	50	2868	5
133	20.5	22.3	0.1407	0.1157	5162	50	5227	10
134	21.4	23.0	0.0714	0.1550	4860	50	3588	25
135	23.4	22.8	0.0404	0.0268	8065	50	4324	10
136	23.7	23.2	0.0696	0.0514	7891	50	6042	10
137	20.9	23.0	0.1436	0.1896	6472	50	4041	25
138	21.3	23.1	0.0386	0.1157	6093	50	5042	25
139	21.3	23.6	0.2282	0.0264	5705	50	4288	5
140	22.5	21.4	0.2332	0.1893	7175	50	4465	25
141	23.0	21.8	0.0714	0.1129	6822	50	4545	25
142	21.1	22.1	0.2287	0.1158	6533	50	6658	10
143	21.9	23.0	0.0421	0.0493	6004	50	6530	10
144	23.5	22.8	0.1418	0.0500	7251	50	4108	10
145	22.5	22.9	0.2275	0.1568	6974	50	3772	25
146	23.2	23.3	0.1446	0.1557	6770	50	3898	25
147	21.6	24.1	0.0721	0.0296	6396	50	5789	5
148	22.5	24.8	0.1482	0.0264	6130	50	3832	5
149	23.0	22.5	0.0429	0.1911	9460	50	5550	50
150	23.2	22.7	0.0693	0.1896	9039	50	4515	50
151	23.5	22.9	0.0354	0.1568	8793	50	4703	50
152	20.5	22.2	0.2279	0.0507	6822	50	6736	5

*3600 square units per square inch.

Table 6. Data for the absorption of methyl mercaptan in water.

Run	Temperature		Displacement Rate		Inlet Sample		Outlet Sample	
	Liquid °C	Gas °C	Liquid cm/min	Gas cm/min	Area*	Range mv	Area*	Range mv
153	21.6	22.5	0.0668	0.1900	6590	50	5929	25
154	20.8	23.5	0.2266	0.0266	6006	50	3888	5
155	22.4	24.1	0.2225	0.0496	5793	50	5947	5
156	22.7	23.8	0.0671	0.1168	5888	50	3613	25
157	23.1	22.7	0.0386	0.0239	6333	50	3294	10
158	23.4	23.1	0.0379	0.1564	6232	50	6193	25
159	24.0	23.5	0.0375	0.1154	5914	50	5113	25
160	24.2	23.8	0.0693	0.1593	5638	50	4536	25
161	21.6	23.4	0.2254	0.1561	7484	50	3765	25
162	22.9	23.8	0.0657	0.0264	5057	50	7656	5
163	21.5	23.9	0.1346	0.1911	7027	50	4730	25
164	22.9	24.2	0.0361	0.1939	6685	50	7598	25
165	19.8	23.1	0.1304	0.1179	5050	50	5234	10
166	21.7	23.6	0.0354	0.0489	4817	50	5463	10
167	21.8	24.3	0.1293	0.0493	4644	50	5013	5
168	22.5	24.1	0.1332	0.1582	4603	50	6052	10
169	22.3	24.6	0.1371	0.0275	4576	50	3063	5
170	20.2	23.7	0.2229	0.1936	4458	50	5752	10
171	21.5	23.6	0.2189	0.1171	4337	50	4012	10
172	23.3	24.1	0.0675	0.0496	4086	50	6272	5
173	22.6	24.4	0.2229	0.0257	7848	25	6419	2

*3600 square units per square inch.

Table 7. Data for the absorption of dimethyl sulfide in various salt solutions.

Run	Temperature Liquid °C	Temperature Gas °C	Displacement Rate Gas cm/min	Displacement Rate Liquid cm/min	Inlet Sample Area*	Inlet Sample Range mv	Outlet Sample Area*	Outlet Sample Range mv	Absorbing Liquid Solution
44	23.8	23.0	0.1239	0.1282	8272	50	6660	10	0.0336 M $FeCl_3$
45	24.1	23.2	0.1993	0.0359	8254	50	6772	25	0.0336 M $FeCl_3$
46	23.1	22.8	0.1278	0.1314	9420	50	4540	5	0.0190 M $HgCl_2$
47	24.0	23.2	0.1986	0.0385	9242	50	8630	10	0.0190 M $HgCl_2$
48	26.5	24.8	0.1307	0.1300	8350	50	7130	10	0.0229 M $CdCl_2$
49	27.1	25.3	0.2014	0.0404	8352	50	7068	25	0.0229 M $CdCl_2$
50	25.0	24.8	0.1279	0.1254	10474	50	8590	10	0.0279 M $CuCl_2$
51	25.9	25.2	0.2018	0.0400	10162	50	8960	25	0.0279 M $CuCl_2$
52	27.1	26.2	0.1278	0.1321	8732	50	3216	25	0.0352 M $ZnCl_2$
53	27.5	26.2	0.2021	0.0361	9308	50	8048	25	0.0352 M $ZnCl_2$
54	25.7	24.9	0.1286	0.1357	8678	50	6840	10	0.0066 M $PbCl_2$
55	26.0	25.2	0.2014	0.0379	8302	50	6756	25	0.0066 M $PbCl_2$
56	25.5	25.6	0.1269	0.1346	7660	50	5950	10	Distilled Water
57	25.8	25.9	0.2014	0.0379	7444	50	5908	25	Distilled Water

*3600 square units per square inch.

Table 8. Data for the absorption of dimethyl sulfide in water.

Run	Temperature		Displacement Rate		Inlet Sample		Outlet Sample	
	Liquid °C	Gas °C	Liquid cm/min	Gas cm/min	Area*	Range mv	Area*	Range mv
233	22.8	24.2	0.2239	0.1679	10075	50	4444	25
234	23.5	24.1	0.1300	0.2029	10608	50	6133	25
235	20.9	21.0	0.0661	0.1629	9326	50	5763	25
236	21.5	21.5	0.1296	0.1611	9181	50	4183	25
237	22.2	22.3	0.0664	0.1257	9049	50	4761	25
238	20.8	23.2	0.1289	0.0279	8981	50	4359	5
239	22.7	23.2	0.2229	0.0286	9043	50	3929	5
240	24.5	23.8	0.1368	0.0532	9155	50	4204	10
241	23.4	24.3	0.0711	0.0521	9233	50	6136	10
242	24.4	24.8	0.0696	0.0279	9249	50	7531	5
243	25.0	24.8	0.0386	0.1268	9274	50	6958	25
244	25.7	25.7	0.0382	0.0543	9250	50	3685	25
245	24.4	25.3	0.2229	0.1279	10023	50	3515	25
246	23.4	24.4	0.0389	0.0279	9682	50	5417	10
247	23.5	24.9	0.2200	0.0518	9540	50	7688	5
248	24.6	25.2	0.0357	0.2050	9584	50	4804	50
249	22.6	25.1	0.2229	0.2039	9652	50	4533	25
250	23.8	25.3	0.1311	0.1250	9933	50	3859	25
251	25.2	25.4	0.0689	0.2057	9857	50	7710	25
252	25.2	24.3	0.0368	0.1671	7905	50	6823	25

*3600 square units per square inch.

Table 9. Data for the absorption of dimethyl sulfide in water.

Run	Temperature		Displacement Rate		Inlet Sample		Outlet Sample	
	Liquid °C	Gas °C	Liquid cm/min	Gas cm/min	Area*	Range mv	Area*	Range mv
273	18.6	22.5	0.0321	0.0511	8872	50	7606	10
274	18.6	22.6	0.1300	0.1239	8855	50	7503	10
275	20.0	22.8	0.0343	0.1639	8952	50	7567	25
276	20.3	23.1	0.0343	0.2004	8760	50	8533	25
277	20.0	23.4	0.0343	0.0293	8820	50	4662	10
278	20.3	23.3	0.0661	0.0268	9255	50	6561	5
279	22.2	22.3	0.0671	0.2000	9259	50	6933	25
280	22.3	23.0	0.1329	0.0282	9292	50	4786	5
281	22.7	23.0	0.2243	0.0279	9485	50	4096	5
282	22.0	22.5	0.2254	0.2007	9777	50	4702	25
283	21.5	22.9	0.1307	0.0500	9670	50	4257	10
284	20.6	23.0	0.1300	0.1661	9774	50	4481	25
285	21.5	23.4	0.0675	0.1657	9065	50	5961	25
286	22.0	23.6	0.0693	0.0507	9160	50	5860	10
287	22.9	22.6	0.2232	0.1232	10503	50	8691	10
288	21.2	23.3	0.2232	0.0500	10208	50	7528	5
289	20.7	23.4	0.0671	0.1250	9289	50	4810	25
290	21.0	23.5	0.1307	0.1982	9300	50	4922	25
291	22.0	23.8	0.0343	0.1250	9428	50	6612	25
292	22.2	23.8	0.2196	0.1632	9242	50	3679	25

*3600 square units per square inch.

Table 10. Data for the absorption of dimethyl sulfide in 0.05 M mercuric chloride.

Run	Temperature		Displacement Rate		Inlet Sample		Outlet Sample	
	Liquid °C	Gas °C	Liquid cm/min	Gas cm/min	Area*	Range mv	Area*	Range mv
253	24.7	24.5	0.0407	0.0282	8144	50	2687	2
254	24.8	24.6	0.1350	0.2039	8240	50	4747	5
255	23.9	24.6	0.0718	0.0286	8495	50	2224	2
256	24.1	24.0	0.1364	0.0268	8573	50	1447	2
257	24.8	24.0	0.0393	0.0518	8636	50	5036	2
258	24.2	24.3	0.2257	0.0529	8582	50	2127	2
259	24.4	24.5	0.2229	0.0289	8627	50	1270	2
260	24.6	24.3	0.0375	0.2011	9319	50	5870	10
261	24.3	23.5	0.0714	0.1254	8354	50	3923	5
262	24.6	23.6	0.1357	0.0511	8378	50	2787	2
263	24.4	23.9	0.2229	0.2000	8329	50	4072	5
264	24.9	24.8	0.0379	0.1689	7937	50	7159	5
265	25.0	24.2	0.1354	0.1271	8150	50	6826	2
266	24.8	24.5	0.0707	0.1682	8111	50	5482	5
267	24.4	23.1	0.0400	0.1230	9015	50	5448	5
268	24.4	23.4	0.0721	0.0521	9014	50	4197	2
269	24.4	23.3	0.0689	0.2004	9640	50	4113	10
270	24.4	23.4	0.2271	0.1239	9432	50	5018	2
271	23.0	21.8	0.2268	0.1621	9257	50	3687	5
272	23.4	22.2	0.1321	0.1643	9309	50	7027	5

*3600 square units per square inch.

Table 11. Data for the absorption of dimethyl disulfide in water.

Run	Temperature		Displacement Rate		Inlet Sample		Outlet Sample	
	Liquid °C	Gas °C	Liquid cm/min	Gas cm/min	Area*	Range mv	Area*	Range mv
177	22.6	25.4	0.0371	0.1268	12271	25	13924	5
178	22.5	25.5	0.2204	0.1268	13192	25	6983	5
179	24.1	25.1	0.1375	0.0521	13685	25	9868	2
180	24.2	24.6	0.0368	0.2021	16332	25	13672	10
181	21.8	23.8	0.2207	0.0529	13765	25	8857	2
182	21.8	23.8	0.1304	0.2004	15255	25	12624	5
183	22.1	24.2	0.2232	0.2018	14981	25	12084	5
184	23.6	24.9	0.0379	0.0532	14721	25	10125	5
185	23.5	25.0	0.1350	0.1250	15619	25	10556	5

*3600 square units per square inch.

Table 12. Data for the absorption of dimethyl disulfide in water.

Run	Temperature		Displacement Rate		Inlet Sample		Outlet Sample	
	Liquid °C	Gas °C	Liquid cm/min	Gas cm/min	Area*	Range mv	Area*	Range mv
186	20.7	24.5	0.2221	0.1675	14820	25	9218	5
187	22.3	24.7	0.0364	0.1654	15365	25	11863	10
188	22.2	24.8	0.1329	0.1289	15793	25	10579	5
189	22.0	24.9	0.1325	0.1682	15140	25	12469	5
190	22.9	25.0	0 0689	0.1243	15101	25	14510	5
191	23.5	23.8	0.0379	0.0279	12729	25	12738	2
192	23.3	23.8	0.0700	0.0286	13150	25	9056	2
193	23.3	24.2	0.1336	0.1982	13858	25	12086	5
194	23.7	24.7	0.0354	0.0543	13837	25	8939	5
195	22.5	23.0	0.0700	0.2032	11545	25	14550	5
196	22.6	23.3	0.2239	0.1989	12466	25	10286	5
197	23.0	24.0	0.2232	0.0536	12361	25	9159	2
198	23.7	24.3	0.0696	0.0529	12389	25	13555	2
199	23.5	24.2	0.2211	0.1264	13826	25	7362	5
200	21.7	24.0	0.2239	0.0282	11729	25	4848	2
201	23.3	24.3	0.1368	0.0539	12413	25	8959	2
202	24.4	24.5	0.0371	0.1268	12896	25	15209	5
203	24.5	24.7	0.0379	0.2021	13119	25	11524	10
204	24.5	25.0	0.0714	0.1711	12278	25	7448	10
205	23.7	24.2	0.1329	0.0279	11694	25	5852	2

*3600 square units per square inch.

Table 13. Data for the absorption of dimethyl disulfide in water.

Run	Temperature		Displacement Rate		Inlet Sample		Outlet Sample	
	Liquid °C	Gas °C	Liquid cm/min	Gas cm/min	Area*	Range mv	Area*	Range mv
206	24.3	24.4	0.0700	0.1654	12633	25	13460	5
207	24.3	25.0	0.2236	0.0282	12334	25	6495	2
208	21.3	24.0	0.2214	0.0511	11006	25	6759	2
209	22.7	24.3	0.1329	0.1243	11516	25	16167	2
210	23.6	24.7	0.2232	0.1679	11111	25	7584	5
211	24.4	24.8	0.0339	0.1646	11643	25	8664	10
212	24.6	24.7	0.0379	0.0289	11425	25	12220	2
213	23.1	23.0	0.1393	0.0268	10060	25	4869	2
214	23.5	23.5	0.0711	0.2014	10850	25	12750	5
215	23.7	23.9	0.1325	0.2004	11257	25	10236	5
216	24.5	24.8	0.1375	0.1682	10892	25	8788	5
217	24.7	25.2	0.2221	0.1261	11240	25	6726	5
218	23.2	23.1	0.0696	0.0500	10451	25	10676	2
219	23.7	23.3	0.0407	0.2018	11201	25	9225	10
220	23.8	24.1	0.2239	0.2034	11879	25	9429	5
221	24.1	23.9	0.0711	0.1221	10510	25	8794	5
222	24.2	23.5	0.0721	0.0279	10439	25	7930	2
223	24.6	24.1	0.1343	0.0518	11022	25	8886	2
224	25.2	24.8	0.0371	0.0536	11308	25	6873	5
225	25.3	24.5	0.0375	0.1239	12138	25	14842	5

*3600 square units per square inch.

Table 14. Data for the absorption of sulfur dioxide in water.

Run	Temperature Liquid °C	Temperature Gas °C	Liquid Displacement rate cm/min	mls. Sample 100 mls avg.	mls. Titrated avg.	mls. I_2 Sol'n	Normality I_2 Sol'n	mls. $Na_2S_2O_3$ Sol'n avg.	Normality $Na_2S_2O_3$ Sol'n
313*	25.1	24.4	0.1395	20.0	10.0	25.0	0.0865	7.7	0.0435
314*	25.0	24.6	0.2261	17.5	20.0	25.0	0.0936	5.2	0.0435
315	24.5	24.9	0.0767	23.0	5.0	25.0	0.0936	15.7	0.0435
316	24.9	25.3	0.0370	21.3	5.0	25.0	0.0936	14.5	0.0435
317	24.1	24.8	0.0385	21.6	5.0	25.0	0.0936	11.9	0.0435
318	24.4	25.2	0.0735	21.8	5.0	25.0	0.0936	16.1	0.0435
319*	22.6	25.5	0.2272	17.0	15.0	25.0	0.1001	9.3	0.0435
320	20.7	25.5	0.1352	17.0	10.0	25.0	0.1001	9.1	0.0435
321	24.9	25.4	0.1363	18.7	10.0	25.0	0.1001	7.5	0.0435
322*	23.0	25.4	0.2240	21.5	10.0	25.0	0.1001	14.5	0.0435
323	22.1	26.2	0.0685	28.5	5.0	25.0	0.1001	3.6	0.0701
324	22.3	26.6	0.0370	24.4	5.0	25.0	0.1001	5.8	0.0701
325	24.0	24.1	0.2209	24.1	10.0	25.0	0.1001	4.0	0.0701
326	22.0	25.0	0.0354	24.6	5.0	25.0	0.1001	5.8	0.0701
327	21.5	25.5	0.1336	16.8	10.0	25.0	0.1001	5.3	0.0701
328	20.9	26.1	0.0707	25.1	5.0	25.0	0.1001	6.9	0.0701

*Gas flow was too low on these runs so liquid level rose in the column.

F. NOMENCLATURE

A_C - cross sectional area; ft^2

a - interfacial surface; ft^2/ft^3

b_1, b_2 - constants

C - concentration; lb Moles/ft^3

$\bar{C}$ - Laplace transformed concentration; lb Moles/ft^3

c_1, c_2 - integration constants

D - diffusivity; ft^2/sec

D_{12} - diffusivity; cm^2/sec

d_c - diameter of wetted wall column; ft

e - Naperian logarithm base

G - superficial gas velocity; ft/sec

g - gravitational force; ft/sec^2

H - Henry's law constant; $(\frac{\text{lb Moles}}{ft^3})_G / (\frac{\text{lb Moles}}{ft^3})_L$

H'_{tOG} - height of a transfer unit; ft

K_{CG} - overall gas mass transfer coefficient; ft/sec

K_L - overall liquid mass transfer coefficient; ft/sec

k_{CG} - gas phase mass transfer coefficient; ft/sec

k_L - liquid phase mass transfer coefficient; ft/sec

k - Boltzmann constant

L - superficial liquid velocity; ft/sec

M - molecular weight

N_A - mass flux of component A; lb Moles/ft^2 sec

N_B - mass flux of component B; lb Moles/ft^2 sec

N_{Re} - Reynolds number

N'_{tOG} - number of overall gas transfer units

N'_{tOL} - number of overall liquid transfer units

P - pressure; mm Hg

P' - pressure; atmospheres

Q - volumetric flow rate; ft^3/sec

r - radius; ft

r_1 - inside boundary radius; ft

r_2 - outside boundary radius; ft

r_{max} - radius at point of maximum velocity; ft

s - surface renewal rate; 1/sec

s - Laplace transform parameter

T - temperature; °K

T_C - critical temperature; °K

t - time; sec

t_e - time of exposure; sec

U - average velocity; ft/sec

V - molecular volume; cm^3/g Mole

V_C - molal volume at the critical point; cm^3/g Mole

W - wetted perimeter; ft

X_A - mole fraction of component A

x - distance; ft

y_A - dimensionless concentration (defined by Equation 24)

$\bar{y}_A$ - Laplace transformed dimensionless concentration

Z - height; ft

α - Bunsen coefficient; vol/vol/atm

Γ - mass rate of flow per unit perimeter; lb/ft sec

δ - thickness of plane of resistance to mass transfer; ft

δ' - thickness of flowing film; ft

ϵ - Lennard-Jones parameter

μ - viscosity; lb/ft sec

μ' - viscosity of solvent; centipoise

ν - kinematic viscosity; ft^2/sec

π - Pi, 3.14

ρ - density; lb/ft^3

σ - Lennard-Jones parameter

φ - surface-age distribution function

Ω - dimensionless function of temperature and potential field

Subscripts:

A - component A

B - component B

G - gas

i - interface

L - liquid

S - solute

1 - component 1 or plane 1

2 - component 2 or plane 2

Superscripts

∞ - bulk stream

$*$ - equilibrium value